Universidad Carlos III de Madrid
School of Engineering

BSc in Biomedical Engineering

DESIGN, CONSTRUCTION AND VALIDATION OF A REGISTERING AND ANALYSIS SYSTEM FOR THE ELECTROPHYSIOLOGICAL PROPERTIES OF AN ISOLATED PORCINE HEART MODEL

Author

Adrián Magaz Molina

Tutor

Andreu M. Climent

June 2015

Hospital General Universitario Gregorio Marañón

Acknowledgements

First of all, I would like to deeply thank Andreu M. Climent, who made it possible for me to start doing an internship at the Laboratory of Scaffolds and Bioartificial Organs of the Health Research Institute of Gregorio Marañón Hospital. Thanks for his motivation, his confidence in me and his patience.

The present project has a great symbolic meaning, the culmination of an important period of my life. I would like to thank all those people who have made it such an unforgettable experience.

To my great friends Miguel, Alba, Gema, Laura and both Celias, and that big family the residence hall Fernando Abril Martorell has been these four years.

To my classmates and colleagues of the degree, the second generation of Biomedical Engineers at Universidad Carlos III of Madrid, for the countless hours that hard work bring together. Thank you for those great moments.

To the people working at LOBA at Gregorio Marañón Hospital. Special thanks to my classmate and lab partner Lidia, who has put up with me all these months and has assisted me in this project.

All the professors, from the different tracks of the BSc. in Biomedical Engineering deserve a special mention as well. For their great seminars and tutorships.

I could not forget my family, special thanks to my parents and brother, for the care and support they have brought all these years, for providing my education and encouraging me to find the right path.

I could not have wished for better people to share my way. Again, thank you all.

Adrián Magaz Molina, June 2015

Abstract

Cardiac fibrillation is as a relevant subject of study in cardiovascular diseases. Its initiation mechanisms, maintenance and interruption processes are still partially misunderstood. Quantifying the complexity of electrocardiographic signals allows researchers to objectify induced modifications by a particular therapeutic treatment. With the aim to study alterations in the cardiac substrate, the objective of this project is to design, build and validate a real-time registering and analysis system for the electrophysiological properties of the epicardial and endocardial tissue of an isolated porcine heart model.

We propose a functional computer user interface. We designed and implemented a platform capable of real-time quantifying electrocardiographic signals. The corresponding methodology consists of the use of a combination of time and frequency domain analysis algorithms divided in separate blocks that work together. While the first block detects the heart rhythm and ECG features according to a Pan and Tompkins based algorithm, the second block detects the fundamental frequency of the myocardial activations based on frequency analysis; and the third one detects ventricular fibrillation episodes based on a phase-space reconstruction of the signal. This system was tested by developing an electrocardiographic waveform simulator. We performed five ex-vivo experiments for validation of the platform using isolated porcine hearts in a Langendorff bioreactor, by means of a controlled backward perfusion of the coronary arteries. Whole-heart optical mapping was carried out as the gold standard, and comparisons between the off-line analysis of the optical recordings and real-time results obtained with the developed platform were made.

Results showed that electrical signals registered with the developed platform were in accordance with dominant frequency maps obtained from the off-line analysis of the corresponding optical recordings. The developed platform was able to real-time differentiate onset of ventricular fibrillation events from sinus rhythm episodes, as well as automatically detect myocardial rhythm and fundamental frequency of myocardial activations.

We conclude that the proposed system is a versatile tool that allows us to easily, quickly and automatically real-timely quantify in a reproducible way electrocardiographic recordings of isolated hearts in a Langendorff bioreactor. This, in turn, would help in the performance of various clinical applications: from ex-vivo studies of the cardiac substrate to the testing of potential antiarrhythmic drugs.

Table of contents

1. Introduction

1.1 Motivation

Cardiac disease is the leading cause of death in Europe and throughout most of the world [1], with arrhythmias being the most prevalent condition. Since cardiac fibrillation is a complex type of arrhythmia whose initiation mechanisms, maintenance and interruption remain partially misunderstood, it is currently a relevant subject of study [2–4]. To fully understand them and develop better therapies, it is crucial to analyze changes in the complexity of fibrillation produced by the use of drugs or maneuvers that alter the myocardium's electrophysiological properties [5,6]. Although laboratory and clinical observations have greatly enhanced our awareness of their mechanisms, a much better understanding of the basics is needed before optimal treatments can be defined [7].

The Unit of Electrophysiology and Arrhythmias within the Laboratory of Scaffolds and Bioartificial Organs of the Health Research Institute of Gregorio Marañón Hospital seeks to uncover the different mechanisms involved in the initiation and perpetuation of cardiac arrhythmias, especially ventricular fibrillation, by mimicking in an ex-vivo isolated porcine heart model the various pathologies associated with abnormalities in the heart rhythm. The final goal is to improve medical diagnoses and treatments. Ventricular fibrillations are induced, and the onset mechanisms are studied: only when you are able to reproduce something, you are able to explain it.

Langendorff bioreactor systems allow us to study ex-vivo the behavior of isolated hearts by a controlled backward perfusion of the coronary arteries, along with optical cardiac mapping techniques that have become a tool of great value for analyzing patterns of activation during fibrillation [8]. However, these cannot give real-time feedback and only provide off-line analysis after experimentation. In this sense, the aim of this project is to develop a versatile registering and analysis electrocardiographic platform for real-time quantification of the signal's complexity that could allow researchers to objectify induced modifications by a particular therapeutic treatment.

1.2 Objectives

The objective of this project is to design, build and validate a registering and analysis system for epicardial and endocardial cardiac electrograms. The application will be used to real-time quantify electrocardiographic signals of the cardiac substrate within the research carried out at the Unit of Electrophysiology and Arrhythmias belonging to the Laboratory of Scaffolds and Bioartificial Organs (Laboratorio de Matrices y Órganos Bioartificiales, LOBA) of the Health Research Institute of Gregorio Marañón Hospital (Insitituto de Investigación Sanitaria del Hospital General Universitario Gregorio Marañón, IISGM).

For the correct accomplishment of the overall objective of this project, the following specific objectives are set:

1. Design, implement and evaluate a registering and storage analysis platform for electrocardiographic signals. The application should have the following properties:

    - Preprocessing of the registered signals.
    - Real-time analysis of the registered signals taking into account both the temporal and spectral information contained in each electrogram.
    - Automatic detection of myocardial activations.
    - Identification of the myocardial rhythm.
    - Automatic detection of the onset of ventricular fibrillation episodes.

2. Design of a waveform simulator to generate epicardial and endocardial signals, used to validate and evaluate the final platform.

3. Validation and evaluation of the system in ex-vivo experiments of isolated porcine hearts in a Langendorff bioreactor: comparative study of the electric signals with gold standard records obtained from optical mapping techniques.

2. Background

This section sets the general basis for the project, and it is divided into a physiological and a technical background. On the one hand, the physiological background covers a literature review of the heart and its electrophysiology as an introduction to the problem of cardiac arrhythmias and ventricular fibrillation in particular. A brief examination of animal models acts then as an opening to explaining the grounds of a Langendorff system required for studying the cardiac substrate of a porcine heart model. On the other hand, the technical background presents how quantification of electrocardiographic signals can be done; both electrical and optical recordings of the electrophysiological activity of the heart are described. The state of the art on signal processing techniques in electrophysiology is presented.

2.1 Physiological background

Electrocardiography

Although Waller was the first one to observe an electrocardiogram (ECG) in 1889, a graph recording the electrical activity of the heart over a period of time [9], it was Einthoven in 1903 that enhanced the technology and made it usable for clinical diagnosis [10].

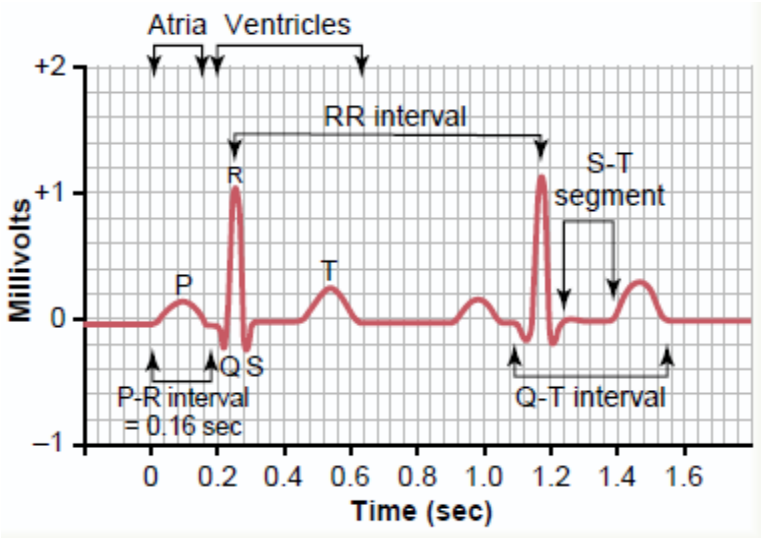

Fig. 1 Schematics of a normal electrocardiogram (ECG). ECG waves: PQRST.

An ECG (Fig. 1) measures the electric pulses generated by a heart, and provides an insight into the control of the timing, synchronization and pumping actions of the organ. The basic pattern of an ECG comprises three waves: P (atrial depolarization), QRS (ventricular depolarization) and T (ventricular repolarization). The correct interpretation of an ECG is complex and requires extensive training, though [11]. Therefore, to understand and interpret ECGs, the relationship between the electric pulses and the heart movements has to be first established.

Anatomy and physiology of the heart

Anatomy of the heart

The heart is a muscular organ that is responsible for pumping blood throughout the body to carry nutrients and oxygen everywhere. The human heart consists of four chambers (Fig. 2) communicated in pairs, with an intermediate partition, known as the atrial septum in the upper chambers and the interventricular septum in the lower ones. These intermediate walls divide the heart in two: the so-called right heart, responsible for receiving deoxygenated blood and pumping it to the lungs, and the so-called left heart, responsible for receiving oxygenated blood from the lungs and pumping it to the organs and tissues of the body [12]. Each half of the heart is then formed by two interconnected chambers: the upper chamber known as the atrium, that receives blood through the veins, and the lower chamber known as the ventricle, responsible for pumping the blood to the arterial network. There are also some valves between the atria and ventricles to prevent back bleeding (the tricuspid valve on the right part and the mitral valve on the left, known as the atrioventricular valves), and at the beginning of the arteries (pulmonary valve on the right side and the aortic valve on the left side, known as semilunar valves) [12].

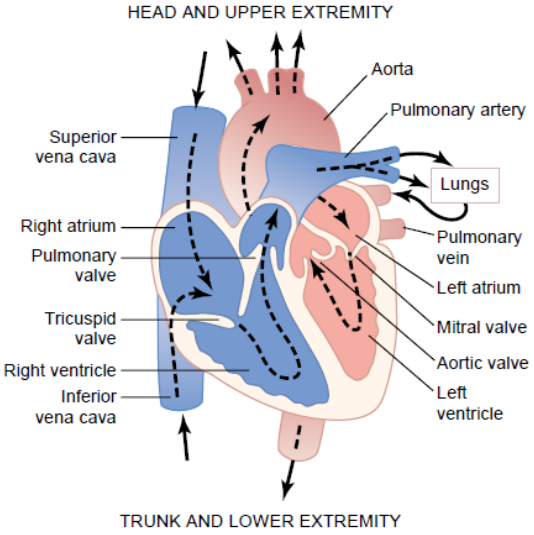

Fig. 2 Structure of the heart, and course of the blood flow through the heart chambers and valves.

Physiology of the heart

From a mechanical point of view, the activity of the heart is divided into two phases: systole and diastole.

The cardiac cycle begins with diastole. At this stage, atrioventricular valves open, allowing blood to flow into the ventricles due to the pressure difference between these and the atria. As the ventricles become nearly full, the flow of blood to the latter gradually slows down in a stage called diastasis. Finally, atrial systole occurs, the stage where the atria contract allowing the blood that still remains in them to reach the ventricles [13].

The second phase of the cardiac cycle is the systole, consisting of an isometric contraction of the ventricles and in which there is no volume but pressure variation, resulting in the closing of the atrioventricular valves. When the intraventricular pressure exceeds that in the arteries (aorta or pulmonary) the semilunar valves open, moment at which the emptying stage starts to take place, lasting about three quarters of the total systole. Blood goes from the ventricle into the aorta until isometric relaxation of the ventricular fibers occur. Consequently, the interventricular pressure diminishes, the semilunar valves close and the atrioventricular valves open, starting this way a new cardiac cycle [13].

Electrophysiology of the heart

The cardiac tissue is an extremely specialized muscle tissue. It consists of cardiomyocytes that are linked together by intercalated disks containing the so-called gap junctions that allow exchange of ions between them and produce a synchronized contraction of the muscle fibers. This mechanical activity is followed by an underlying electrical activity that is responsible for maintaining synchronism.

The difference in net charge between the intracellular and extracellular environments of the cell causes a potential difference between the inside and the outside known as the resting potential, and that in cardiac cells is approximately -90 mV (taking the outside of the cell as reference).

Some cells (including cardiomyocytes and neurons) are excitable, meaning that they are able to produce and respond to electrical signals, autonomously increasing the resting potential due to an external stimulus and generating what is known as an action potential. Action potentials have at least three distinct stages [14] (Fig. 3):

- **Depolarization**: during this stage, the charge within the cell rapidly shifts from negative to positive, initiating the action potential. It is due to a quick inflow of Na+ ions.
- **Plateau**: the inflow of Na+ ions stops, but a balance is maintained between the inward movement of Ca2+ ions and the outward movement of K+ ions. During this stage the net charge is almost null and the action potential is maintained constant. The cardiomyocyte cell is contracted too due to the inflow of Ca2+ ions.
- **Repolarization**: Ca2+ channels are closed, while K+ channels remain open. This causes the cell to repolarize, so the action potential is brought back to the **resting state**.

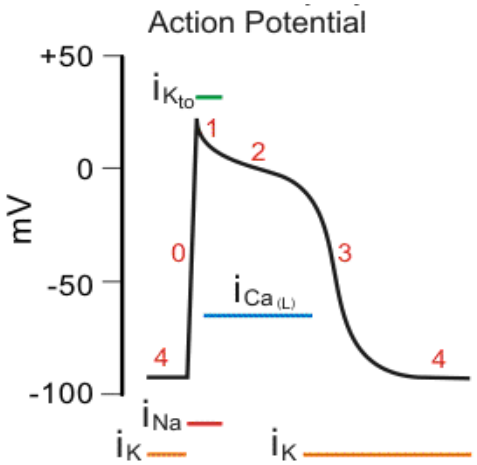

Fig. 3 Action potential of a cardiac cell. Four clear stages are present. Phase 4: resting membrane potential; Phase 0: rapid depolarization of the cell with inflow of Na^+; Phase 1: initial repolarization with outflow of K^+ and Cl^-; Phase 2: plateau with inflow of Ca^{2+} and outflow of K^+; Phase 3: rapid repolarization with K^+ out.

For the action potential to be triggered, an external stimulus is needed, except for those cells that are self-excitable. This stimulus can be simulated in the laboratory by injecting a current in the cell by means of an electrode, but in the natural state, the stimulus of a cardiomyocyte comes from an adjacent cell. Thus, when a cardiomyocyte is depolarized, it stimulates its neighbors, and these, if stimulation is sufficient, depolarize and stimulate in turn theirs. This way, the electric impulse is transmitted throughout the myocardium in a very short period of time, and the heart muscle contracts in a synchronized way [15].

The cardiac activation responsible for the initiation of the heart beat under physiological conditions is generated in a structure located in the right atrium and made up of self-excitable cells, known as the sinoatrial node (SA). The stimulus propagates from the SA node to the atrioventricular node (AV) in the interatrial septum, at which point the signal suffers a delay to allow the full blood refill of the ventricles. The stimulus then diverges and propagates along the right and left bundle of His to the respective Purkinje fibers in each side of the heart (see Fig. 4). These are special conducting fibers larger than cardiomyocytes and with the ability to conduct signals faster and more efficiently, allowing the ventricles to simultaneously excite and contract. This corresponds to the normal rhythm of the heart, the sinus rhythm (SR) [16].

Another characteristic feature of self-excitable cells is the refractory period (RP), the interval of time during which another action potential cannot be initiated (around 250ms in ventricular cardiomyocytes), meaning that the cell cannot be re-excited. This avoids generation of reentrant excitation circuits that may end up in arrhythmias.

Cardiac arrhythmias

As previously explained, the electrical stimulus that causes myocardial contraction spreads throughout the heart muscle causing it to contract in a synchronous way. Under normal circumstances (Fig. 4), the SA node is the natural pacemaker that controls and regulates the pulse rate. At the beginning of each cycle, it generates electric impulses to cause the atrium to pump blood. But if impaired, its function is taken over by other parts of the heart [14]. The loss

of such synchronism causes a series of pathological situations that fall under the name of arrhythmias.

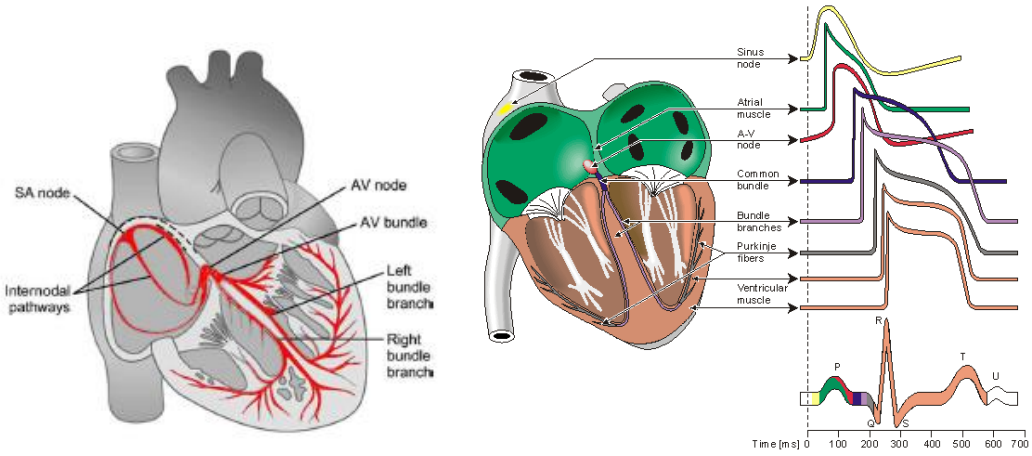

Fig. 4 Activation sequence and action potentials in the genesis of an electrocardiogram under NSR.

Fibrillation is the most dangerous kind of arrhythmia since it causes a contraction of the myocardium in a completely uncoordinated way, resulting in a totally inefficient mechanical activity. These can occur either in the atria or in the ventricles [17]. The former one is not fatal, but it carries serious implications since it results in an increase of the ventricular rate, and in those ventricular areas where blood accumulates it can generate a thrombus that might later travel through the bloodstream. In ventricles, consequences of fibrillation are much more dangerous [4,18]: the systolic pressure is totally ineffective, and as consequence, the blood pressure drops. This decrease causes a lack of oxygen in all organs, including the heart itself. Ventricular fibrillation causes death within minutes if not reversed by an electric shock. Therapy for control of fibrillation includes drugs, pacing or ablation of the heart tissues. Therapeutic maneuvers include surgical or radiofrequency catheters that induce linear lesions to reduce the atrial/ventricular tissue and prevent requisite number of reentrant wavelets [17].

During fibrillation (Fig. 5), myocardial activation is extremely heterogeneous and complex. This has led to the widespread belief that it is the result of a completely random process. In fact, traditional theories are based on Moe's hypotheses [19] in which fibrillation is the result of multiple activation wavefronts that move erratically resulting in excitation patterns that are highly irregular. Nevertheless, the recent application of the theory of nonlinear dynamical systems to the study of fibrillation [20], together with cardiac mapping techniques of high resolution, have led to the believe that fibrillation is a problem of self-organization of nonlinear electrical waves with both a deterministic and a random component [3].

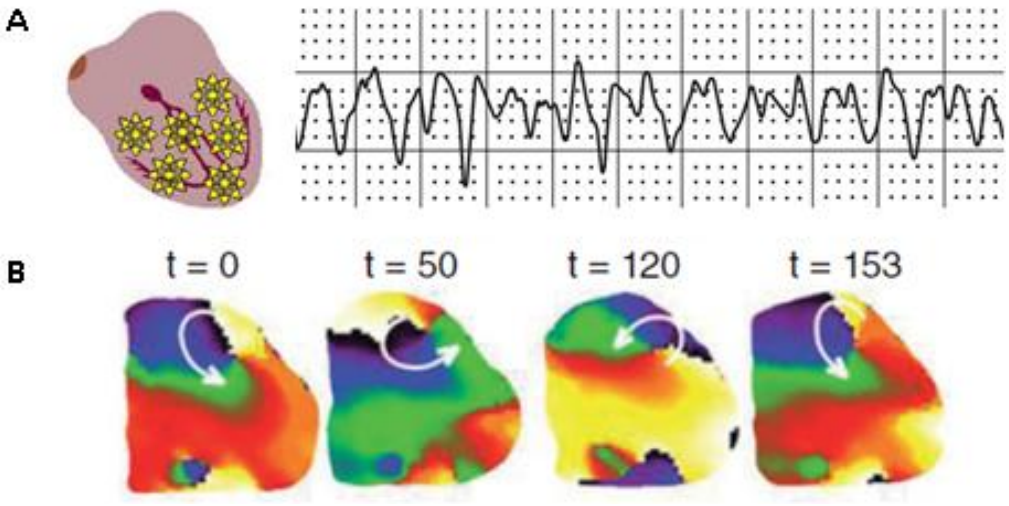

Fig. 5 A: Chaotic ventricular depolarization and electrocardiogram during ventricular fibrillation. **B:** Ventricular fibrillation in a human heart: four action potential phase snapshots depict a rotation of spirals with vortex-like reentry, with white arrows marking its location and direction. Taken from Basic Cardiac Electrophysiology for Physicians [14].

Animal models

Within cardiovascular diseases, the use of animal models has substantially contributed to the knowledge of pathogeneses and has helped in the development of diagnostic techniques, as well as in the validation of preventive and therapeutic procedures [21].

Although animal models fail to completely resemble the actual observed data in the clinic, they do allow the obtaining of direct information of certain phenomena by means of a proper control of variables and use of precise procedures. However, the latter are often invasive and difficult to be eligible in clinical studies. The main advantages of these types of models are the possibility to use controls, and set conditions that otherwise could affect the results by varying one or more factors. Within the drawbacks, there exist differences between the human pathology and the experimentally induced disease, produced among other things, by differences in regulatory genetic mechanisms or in those factors that determine the cardiac and vascular properties [22].

Although significant insights into cardiovascular biology have been made plausible thanks to small animal models, differences exist on heart rate, oxygen consumption or physiological responses. Larger animal models, such as pigs, resemble more closely the function, anatomy and physiology of human beings. In fact, porcine hearts exhibit coronary artery anatomy and gross anatomy structure similar to that of humans [23].

Langendorff system

When researching on animal models, the isolated heart model is a working method widely used. The organ is maintained alive while its electrophysiological parameters remain stable and well-controlled [24]. To this end, the use of a perfusion system is widespread. It was Oscar Langendorff in the early 1900s who pioneered in the development of the first isolated perfused system for mammalian hearts, later known as the Langendorff system [25].

The Langendorff system is designed to perfuse isolated mammalian animal hearts such as those of mouse, rat, rabbit or guinea pig, using the Langendorff technique, while providing in-vitro measurements, maintenance and control of multiple circulatory parameters: from cardiac electrical activity to pressure, temperature or flow rate that can be later processed to allow researchers to monitor heart function in a close-to-physiological environment [26], and extend the cardiovascular knowledge regarding the fundamental pathophysiology of the heart or in the study of pharmacological inhibitors.

How it works

Since its invention, this bioreactor has proven to be an invaluable source in the current understanding of the basic physiology of the heart [26], and it certainly continues to be widely used at present because of its effectiveness and simplicity. Its general functioning has been maintained from the time of its creator, being the heart of the mammal perfused by cannulating the aorta. Only some improvements on the control of temperature, pressure and oxygenation have been made.

Under normal cardiac contractions, oxygenated blood flows out of the left ventricle into the aorta, with an ostium (hole) feeding blood into the coronary arteries. In the Langendorff system, however, a buffer solution is forced retrogradely down the aorta opposite to the normal physiologic blood flow [26]. This way, the aortic valve is closed under pressure, preventing the perfusate to enter the left ventricle but being forced through the ostia into the coronary bed, thus maintaining the availability of the heart muscle. After going through the coronary vascular system, the oxygenated buffer solution is drawn off via the coronary veins to the coronary sinus and into the right atrium, finally flowing out via the right ventricle and pulmonary artery, tending to drip from the apex of the heart and making it easy for collection.

Advantages / Disadvantages

The use of an isolated heart for experimentation has some fundamental advantages, which although might distance the model from reality, allows to have certain control of the physiological parameters. On the one hand, cardiac perfusion does not depend on the effectiveness of the mechanical activity of the heart; this allows prolonged studies of the pathological conditions that would otherwise result in the death of the animal, such as long-term ventricular fibrillation [24]. On the other hand, it allows studying the cardiac events without neurohumoral interference because the heart is separated from the vegetative innervation [27]. Based on these features, highly reproducible results can be obtained.

Although this system was a breakthrough in the study of the heart's physiology and it is still widely used today [24], it presents some limitations too. As the heart contracts without performing work and the aortic pressure is kept constant, a coronary flux higher than normal is obtained. However, there are variants in which, by means of various devices, the heart contracts with a given load [27]. Furthermore, although the perfusate nutrient solution that is used attempts to mimic the blood plasma, it does not contain proteins, natural ions, hormones or other molecules found in blood. This makes the electrophysiological stability, and therefore, the life of the heart, to be limited to a few hours [26].

The system

The average Langendorff system (Fig. 6) consists of peristaltic pumps, an oxygenator, a roller pump, a heat exchanger, a heart chamber and transducers, and a water-jacket system with warm circulating water for precise temperature control of the perfusate and of the heart at 37ºC [24]. Peristaltic pumps deliver the perfusate media from the reservoir, where it is continuously gassed with a mixture of carbon dioxide and oxygen [28], and supplies it with a constant perfusion flow to a heat exchanger reservoir chamber where it is maintained at 37ºC. This, in turn, is connected with an aortic cannula into the heart.

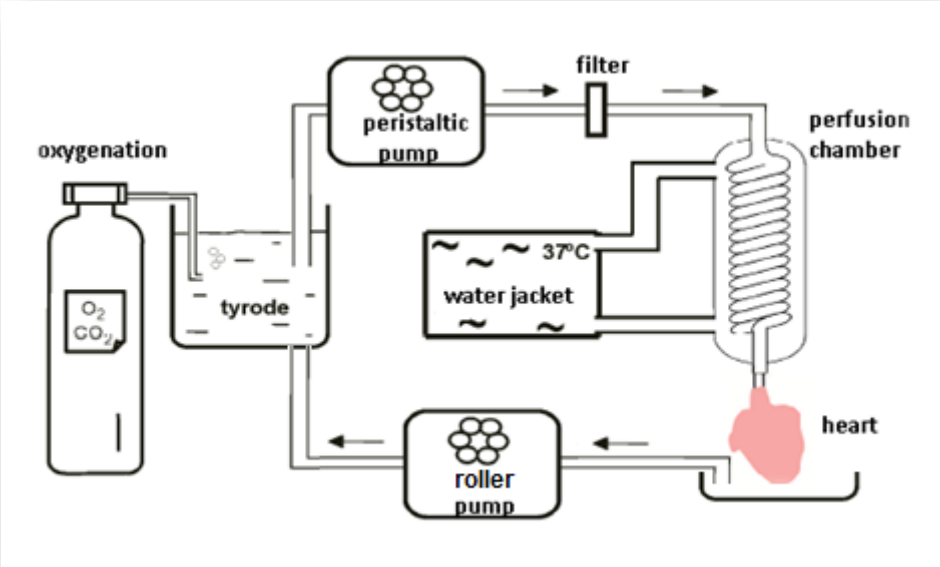

Fig. 6 Schematics of a Langendorff set-up: the perfusate solution is oxygenated and pumped to the aorta of the heart by means of a peristaltic pump as it goes through a filter. A pressure valve for regulation, a water jacket system for temperature regulation and a roller pump for the supernatant to return to the reservoir tyrode chamber.

The Langendorff system can operate in two modes of retrograde heart perfusion [24], though: either in constant flow or in constant pressure mode.

- In **constant pressure mode**, the perfusate is driven to the cannulating aorta of the heart by a constant hydrostatic pressure created by a set height column of fluid. For example, by positioning a reservoir and its fluid meniscus a known distance above the tip of the perfusion cannula. This represents the cheapest and simplest set-up of the Langendorff system [24,26].
- In **constant flow mode**, the perfusate is driven to the cannulating aorta of the heart, pumped with the set desired flow rate and administered by a peristaltic pump. It is ideal where reliance upon the heart's auto-regulation of the coronary tone is required [24,26].

In addition, supplementary devices like constant flow/pressure devices or ECG sensors can easily be added to the system.

The perfusate medium is usually made of a saline solution without cellular or protein content, buffered and with the necessary amount of glucose as the metabolic substrate to at least mimic blood's viscosity. The ionic components might vary, being potassium and calcium the most variable.

2.2 Technical background

A technical overview of the recording techniques used for acquisition of the signals is provided, as well as some of the most common signal processing algorithms in electrophysiology.

Signal acquisition methods

Regarding the recording of the electrical activity of the heart, there are two major groups: electrical and optical recordings.

Electrical recordings

Electrical recordings are based on measuring the potential difference between two points, meaning the electric current flowing between them. For instance, electrograms are widely used in the clinic as a non-invasive approach.

Due to the fact that electrocardiography signals vary from the microvolt to the minivolt range and that they are usually subjected to various sources of noise and interference (both external and internal), electrical recordings of ECG signals are based on the use of an electronic circuit (Fig. 7) intended for amplification and filtering of the signal for better interpretation.

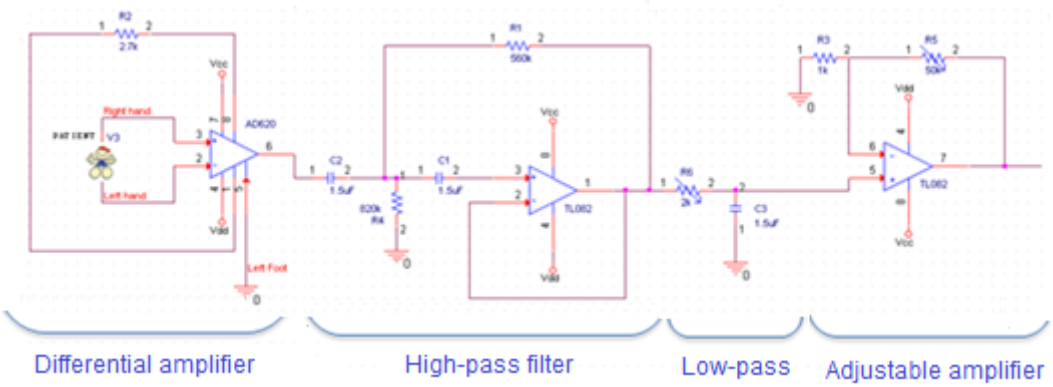

Fig. 7 Basic electrocardiogram circuit: amplification and filtering stages.

A basic electrocardiogram circuit consists of two majors stages: amplification and filtering.

- **Amplification**. The amplification step is mainly implemented through a differential amplifier to make sure noise from the inputs is not amplified. The output impedance should be low to drive any external load with minimal distortion, and the gain should be typically large. A high common mode rejection ratio to eliminate large offsets is usually required too. An instrumental amplifier is usually used to fulfill such characteristics by

amplifying the difference between two input terminals and rejecting the common signals between them.

- **Filtering**. The ECG bandwidth usually ranges between 0.5 and 30Hz, and filtering is typically done through a combination of low-pass and high-pass analog filters.
    - The low-pass filter provides the upper cutoff of the bandpass to eliminate any unwanted signals (i.e myocardial artifacts).
    - The high-pass provides the lower cutoff frequency (i.e removal of breathing artifacts).

Optical recordings

Optical recordings provide a measurement of the action potential between the inside and outside of the cell's membrane, achieved by optical mapping techniques. In the case of the heart, understanding how electric waves spread through its anatomy (Fig. 8) is critical to understanding normal impulse propagation and cardiac arrhythmia mechanisms [29].

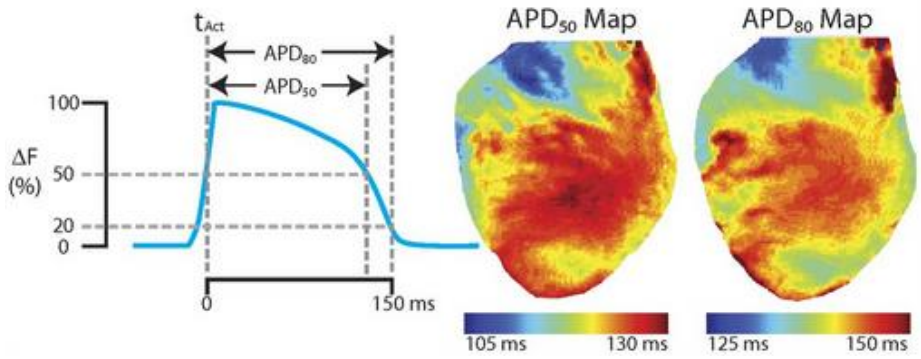

Fig. 8 Optical mapping for measuring the Action Potential Duration (APD). Taken from [30].

Optical mapping is based on the use of fluorescent molecular probes to transduce electrical events into changes in light intensity, and depends on the physical principles of wavelength-dependent light-tissue interaction [31]. It requires filters and light sources to illuminate the cardiac tissue treated with a fluorescent probe, and a detector to sense the changes in fluorescent intensity [29].

- **Filters:** Optical filters are used to reduce background light, decrease the probability of photobleaching and allow selected wavelengths of light to reach the detector [32] .

- **Light sources:** Light sources are responsible for excitation of the fluorescent dyes.
  The perfect light is a monochromatic laser light [32], although light-emitting diodes (LEDS) are an attractive alternative too: they consume very low power and produce fewer imaginary artifacts, but above all, they are cost-effective, portable and easy to use [29], and allow for complex and rapid wavelength switching.
  Because continuous illumination results in photobleaching, the sample is usually kept in the dark and only enough light is used to get the required image [32].

- **Fluorescent probes:** Voltage sensitive dyes (i.e styryl dyes such as di-4-ANEPPS) are the most popular in optical mapping [32]. They consist of organic molecules that bind with high affinity to the outer layer of the cell bilayer membrane of cardiomyocytes, and

change their spectral properties in response to changes in the membrane potential. When excited by a light source with an appropriate light excitation wavelength α1 (corresponding to the dye's absorption spectrum), dye molecules fluoresce light (by emitting photons) with a determined wavelength α2 longer than that of the excitation, and to a greater or lesser extent in proportion to the transmembrane potential of the membrane [33,34]. This provides optical signals that mimic action potentials of the cells, and allow for visualization of activation and recovery processes of the region under study (Fig. 9).

The newest optical mapping techniques allow measurements of more than one fluorescent probes. For example, calcium sensitive dyes (i.e rhod-2 AM) bind to Ca^{2+} molecules within the cells, and when excited with a proper light wavelength will fluoresce in proportion to the calcium efflux from the sarcoplasmic reticulum (Ca^{2+} ion concentration). Therefore, simultaneous measurement of both action potential and calcium propagation is vital to provide insight into arrhythmic processes.

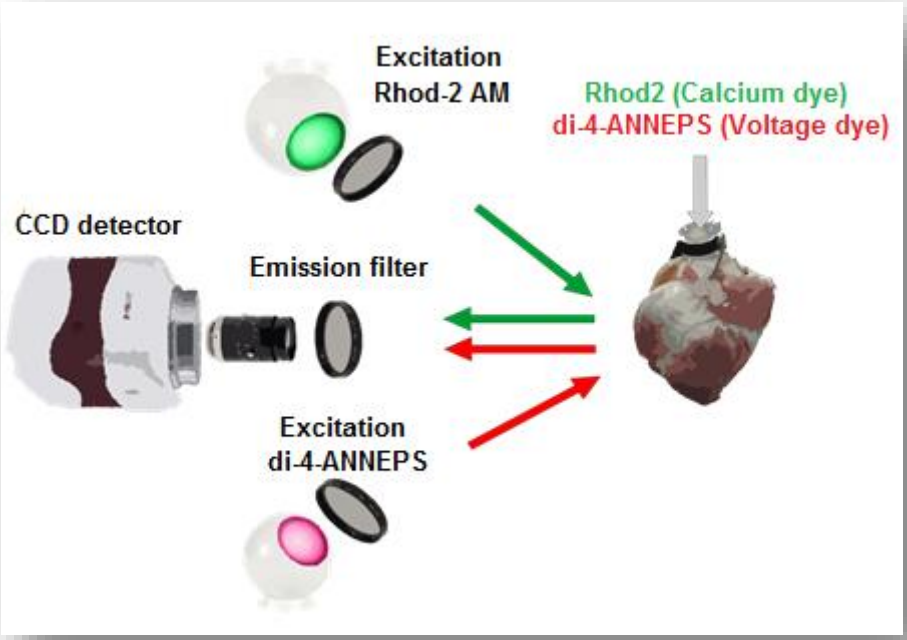

Fig. 9 Simplified optical mapping set-up: CCD camera, emission filter and LED source lights. Excitation and emission of the tissue sample.

- **Detectors**: The most widely used photo detector is a charged-couple device (CCD) camera [35]. A CCD video camera is a semiconductor device segmented into an array of 10^6 or more light sensitive recording pixels. In this sense, CCD cameras provide high spatial resolution [36]. They are in charge of quantifying the amount of emitted fluorescent light. When a photon hits a pixel, electrons are released and an increase of charge in the pixel is produced. The generated charge is collected over an interval, and then converted to a video signal comprised of voltages. Each interval corresponds to a single frame, and each frame represents the light collected by all pixels over the same interval [32].

Optical mapping techniques offer higher resolution to study the electrical activity of the heart [29] and they are used as the gold standard procedure; no real-time feedback is possible though, and they can be currently used only in in vitro pre-clinical studies: the fluorescent probes used remain toxic and might target cells other than cardiomyocytes.

Signal processing in electrophysiology

To date, there exist numerous mathematical algorithms in the scientific literature for analysis of the different complexities of ECG signals. They are based on time or frequency domain, or even in a combination of both [37]. Some of the most common ones are briefly described below:

Time-domain analysis:

- *The Standard Exponential algorithm***:** The STE algorithm [38] is based on counting the number of crossing times of the ECG signal with and exponential function decreasing on both sides. There is also a modified version that lifts the decreasing exponential curve at the crossing points onto the following relative maximum, giving rise to better detection results.
- *Tompkins***:** The TOMP algorithm [39] is based on the search of QRS complex in the time domain, using slope, amplitude and width information.
- *Scattered plots:* Scattered plots can also be used for ECG discrimination [40], but analysis of ECG morphology is not possible.
- Template matching and cross-correlation algorithms:
    - *Threshold Crossing Interval*: The TCI algorithm [37,41] operates in the time domain, where decisions are based on the position and number of times the ECG signal crosses a certain detection threshold.
    - *The Auto Correlation Function*: The ACF algorithm [42] finds repeating patterns at different points in time by means of cross-correlation and based on analyses of periodicities within the ECG. In theory, it allows to separate VF from SR based on aperiodicity/periodicity of the signals, but the problem lies in the assumption that VF signals are always aperiodic.
    - *The Complexity Measure algorithm:* The CPLX algorithm [43,44] transforms the signal into a binary sequence and searches then for repeating patterns.
    - *Signal Comparison:* The SCA algorithm [37] operates in the time domain comparing the ECG with predefined reference signals, and makes decisions based on residuals. However, results are not always expected.
- *Time-delay phase-space reconstruction algorithm:* The PSR algorithm is based on the analysis of the signal's phase, using the Hilbert transform to reconstruct the so-called phase-space diagram.

Frequency-domain analysis:

- *The Spectral algorithm:* The SPEC algorithm [45] operates in the frequency domain. Based on analyzing the energy content of the signal in different frequency bands by means of the Fourier Transform, decisions are made according to certain thresholds. VF, VT and SR can be differentiated.

Time-Frequency domain analysis:

- *Wavelets:* The use of wavelet analysis for discriminating ECG signals is currently one of the most promising algorithms. The wavelet transform of a signal may be represented both in the frequency and time domain, by decomposing the signal into different elements and analyzing each one of them [46].
- There exist a variety of other time-frequency processing techniques that could be modified for its applicability in ECG analysis (Wigner distribution, Rihaczeck and Margenau-Hill, Choi-Williams, Page representation and so on [47]), but we are not going into detail. The spectrogram or the scaleogram in wavelet analysis are other examples too.

Most times, a single algorithm for both ECG discrimination and morphology analysis of its features is not possible, and a combination of approaches is usually performed. As seen, different algorithms have been implemented over the years, but in this present project, both a real-time and frequency analysis of the signals will be performed.

Since one of the objectives within this project is to develop a real-time registering and analysis platform able to detect myocardial rhythm, myocardial activation and onset of ventricular fibrillation episodes, the following algorithms will be used: a TOMP based algorithm for identifying myocardial rhythm, a spectrum analysis for detection of the fundamental frequency of myocardial activations, and a phase-space reconstruction algorithm for onset detection of ventricular fibrillation episodes. The main reasons are due to versatility of the system: both a TOMP based algorithm and a spectrum analysis are simple in terms of computation time and its accuracy is good. For quantifying fibrillation, the phase parameter is the most suitable one; amplitude is often ambiguous and prone to acquisition artifacts, while frequency has limitations in tracking temporal variations [48].

Such analyses allow appreciation of both the evolution of the signal over time (temporal analysis), as well as the frequency components the signal contains (spectral analysis). A dynamic analysis of the signal can be carried out this way.

TOMP based algorithm

The Pan and Tompkins algorithm [39] is based on a sequence of three processing stages: linear digital filtering, nonlinear transformation and decision rule algorithms.

The linear digital filtering stage is intended to emphasize specific features of QRS complexes, while reducing false positives. It mainly consists of a bandpass filter, a derivative filter and a moving average integrator. The bandpass filter helps reduce interferences in the ECG signal due to muscle movements and the 60 Hz interference, or noise regarding the baseline wander and the T wave. In normal conditions, the QRS energy is maximized in the passband 5 to 20 Hz. Differentiation of the signal provides information about the slope of the QRS complex, and the purpose of the moving integrator is to obtain additional waveform feature information to that of the slope of the R wave: long duration and large amplitude QRS waves in the signal might be found, and only the slope of the R wave cannot detect such waves.

The nonlinear stage corresponds to the squaring of the signal, which intensifies the slope of the frequency response curve and helps restrict false positives caused by T waves with higher than usual spectral energies.

Adapting thresholding operations and refractory periods are taken into account for validation or elimination of QRS complexes, as opposed to high-sloped T waves or noise artifacts. No QRS complex can occur if it lies within the refractory period of 200ms after a previously detected one.

The spectral analysis

The QRS complex in ECG signals varies with the origin and the conduction path of the activation pulse. When the activation pulse does not travel through the normal conduction path, the QRS complex becomes wide, and the high-frequency components are attenuated [49].

For frequency-based features, frequency spectrum of individual QRS complex (Fig. 10) is found in the range of 0–20 Hz, while frequencies of ventricular fibrillation signals are usually concentrated between 4–7 Hz [50] and the amplitude of the spectrum decreases as the frequency increases [51].

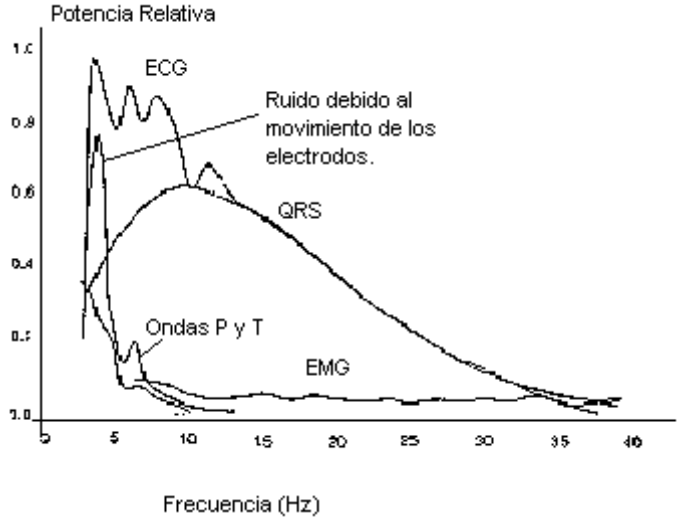

Fig. 10 Frequency component of an ECG-EMG signal

Based on these features, frequency analysis of the signals can be performed, and the fundamental myocardial activation frequency can be calculated.

The phase-space reconstruction algorithm

To date, few studies have been carried out regarding detection of cardiac fibrillation due to the high irregularity of the signal and the inability to get a determined pattern to detect [47]. It is not easy to differentiate it from other pathologies; detection is complicated because of the presence of noise generated by external agents to the heart that contaminates the signal and hinders its analysis. Despite this, phase analysis can be used as a method to quantify and discriminate the spatiotemporal organization of electrograms, to discriminate ventricular fibrillation episodes from normal sinus rhythm ECGs by representing the non-linear characteristics of the dynamic systems.

If fibrillation is not a random process and shows temporal organization, then it is possible to demonstrate that future or present time samples x(t) in an electrogram are dependent on past ones x(t−τ), and this relation can be graphically visualized in a two-dimensional phase-space plot [48]. For an unlimited number of precise data without noise, it is possible to choose any lag time τ. But in the case of working with experimental data, interferences and noise are always present, and only a finite number of data with finite precision can be measured based on the acquisition system. Therefore, features of the reconstructed phase-space would depend on the chosen value of τ. If τ is too small, then x(t−τ) is too close to x(t) and the phase space is too decreased around the diagonal. If instead τ is too large, geometrical deformation of the phase portrait may occur [52] (Fig. 11).

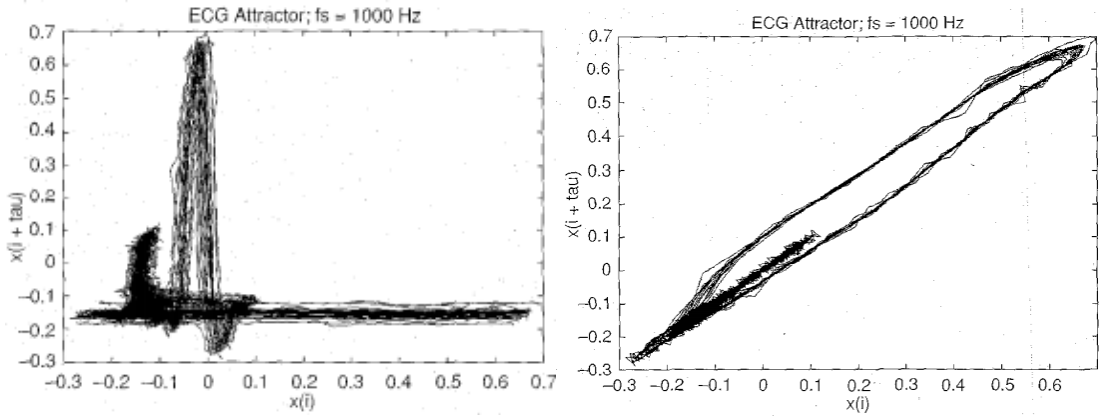

Fig. 11 Reconstructed attractors of an ECG signal with long-time lag τ=120 (right) and with short-time lag τ=2. Taken from [52].

In this approach, and instead of using a time-delay version of the electrogram, the phase-space reconstruction algorithm is based on a method that uses the Hilbert Transform to reconstruct the so-called phase-space by generating a phase shifted signal.

The Hilbert Transform [53,54] is a linear operator used in signal processing that takes a real signal x(t) and returns a helical sequence, sometimes called the analytic signal z(t). The analytic signal $z(t) = xr(t) + ix_H(t)$ has a real part xr(t), which is the original data, and an imaginary part $ix_H(t)$, which is the Hilbert transform of x(t). The imaginary part is a version of the original real sequence with a 90° phase shift.

The Hilbert transform $x_H(t)$of a signal x(t) is defined by:

$$(1) \qquad x_H(t) = \frac{1}{\pi} P.V \int_{\infty}^{\infty} \frac{x(\tau)}{t-\tau} d\tau,$$

where PV means that the integral is taken in the sense of the Cauchy princple

It can be seen from (1) that the Hilbert transform can be considered as the convolution of the functions $x(t)$ and $\frac{1}{\pi t}$. Due to the properties of convolution, the Fourier Transform XH(w) of $x_H(t)$ is the product of the fourier transforms of x(t) and $\frac{1}{\pi t}$. Thus, for w>0, XH(w) = - iX(w) and for w<0,

XH(w) = iX(w). This means that the Hilbert transform can be realized by an ideal filter whose amplitude response is unity and phase response is a constant $\frac{\pi}{2}$ lag at all frequencies w>0.

The Hilbert Transform series has the same amplitude and frequency content as the original sequence and includes phase information that depends on the phase of the original signal [54].

3. Methods

This section describes the hardware and software interconnections followed to carry out the experiments and real-time data acquisition and analysis of the signals. The ECG registering and analysis platform developed during this project will be fully presented, and the validation strategy will be described (Fig. 12).

Two different approaches for evaluating the correct performing of the system have been carried out: (1) to develop an electrocardiography waveform generator for mimicking the signal acquisition environment in the Langendorff system, and (2) to perform ex-vivo isolated heart experiments where the developed platform has been used, and results obtained from the signal processing algorithms have been compared to those from the gold standard whole-heart optical mapping.

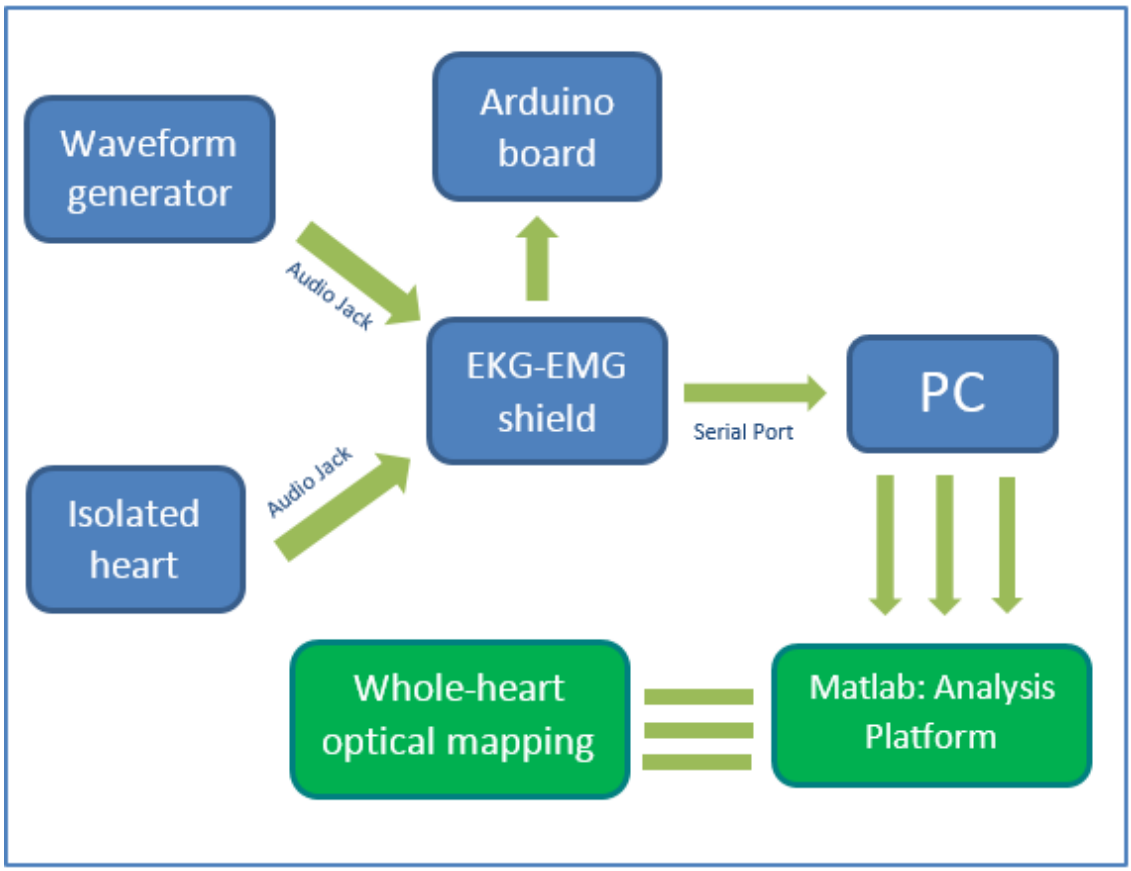

Fig. 12 Flowchart of the project.

3.1 Acquisition and registering system

A shield EKG-EMG board (Olimex) (Fig. 13) was stacked on top of an Arduino Mega2560 for setting the acquisition system of the signals.

An Arduino Mega2560 was used in this stage due to its processing capacity that allows for a higher sampling frequency thanks to a faster transmission speed with the PC. Another reason why such model was chosen is due to its multiple I/O analog and digital pins that might allow a future extension of the project.

The shield EKG-EMG board is a stackable modular peripheral circuit that piggybacks onto the Arduino device and supplies it with extra functionalities, in this case, for acquiring, amplifying and filtering biopotential signals originating in the heart.

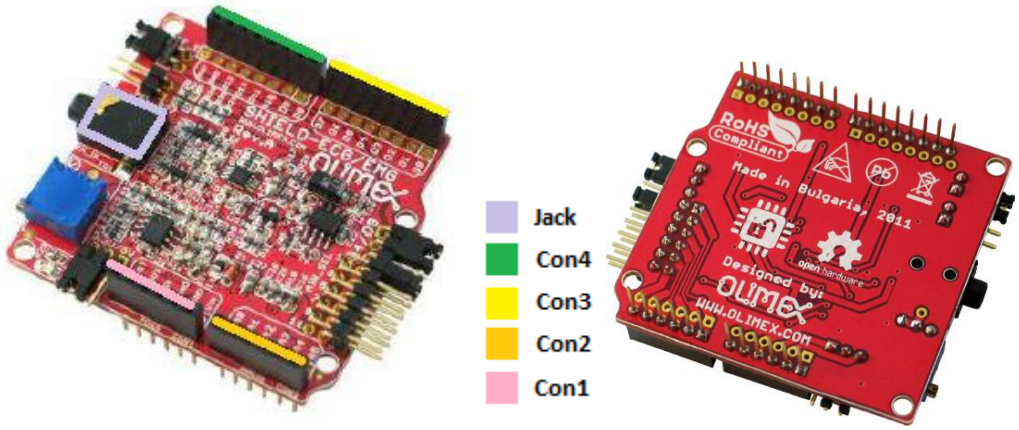

Fig. 13 Shield-EKG-EMG board: upper view and lower view of the board

The jack connection of the board (see Fig. 13) allows signals to be acquired with an input source: a catheter in the case of the isolated heart, or directly from the waveform generator. In either case, an audio-jack clip was welded to the input source: the current flow of electrodes was taken into account; and the GND, positive and negative channels of the clip were borne in mind. Everything was isolated with polymer plastic to reduce noise and artifacts.

The input connected by the jack to the EKG shield collects the data and transmits it to the shield, where it is received by Con2 (see Fig. 13) and converted from analog to digital information:

- First, the data is tested according to its voltage and frequency: the EKG shield is protected against high voltage currents, and will reject any high frequencies since electrocardiographic signals are intended to be frequency-low (Fig. 14).
- The signal is amplified 10x, and frequencies lower than cutoff frequency 0.16 Hz are attenuated (Fig. 14). This is done to remove breathing artifacts that may distort the input signal.

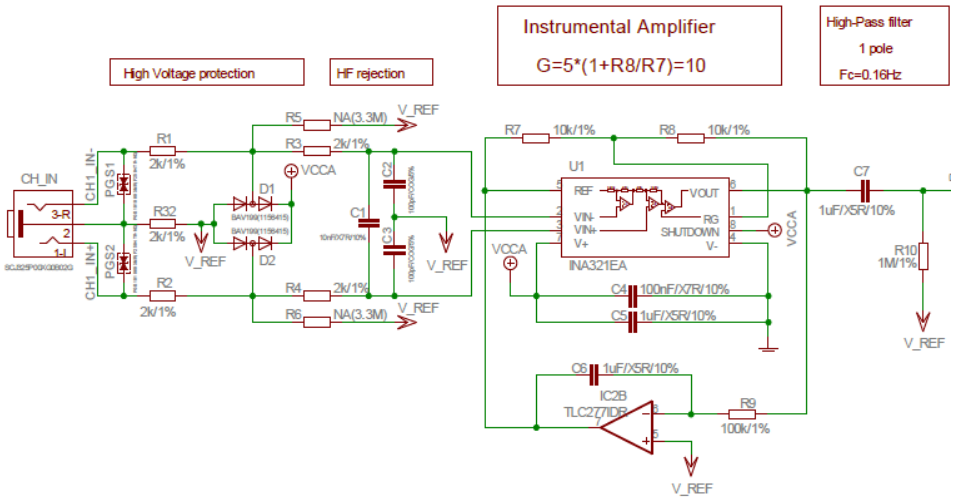

Fig. 14 Simplified overview of the internal circuit of the EKG-EMG board: 1st and 2nd stages.

- Due to the filtering of the signal, not only noise is being attenuated but also the signal itself is being diminished. The signal must then be amplified a second time (adjustable gain between 5.6 and 101), and only frequencies above 0.16 Hz are allowed to go through (Fig. 15).
- Finally, the signal goes through a third order Bessel filter with a cutoff frequency of 40 Hz to remove noise from the power supply, and amplified 3.56x arriving at Con2 (Fig. 15).

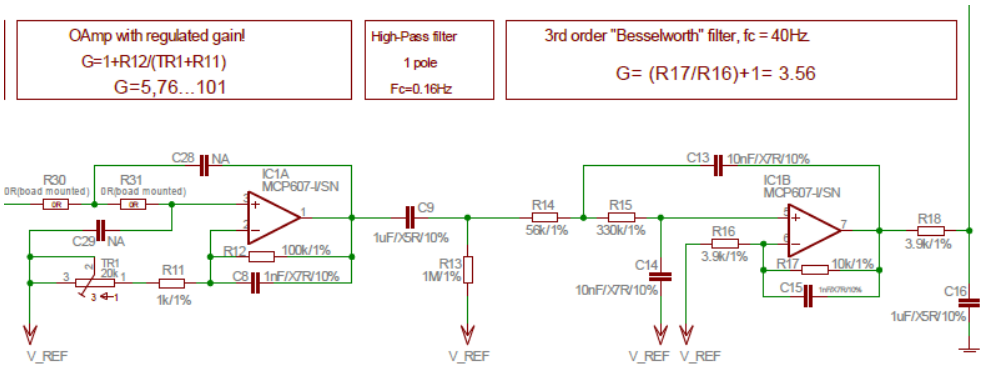

Fig. 15 Simplified overview of the internal circuit of the EKG-EMG board: 3rd and 4th stages.

In this sense, the digital signals flow from the EKG-EMG board, where they are acquired, analog converted and pre-filtered, to the Arduino board where they are sent through a Serial Port to the PC for further processing in the analysis platform: the connection of the Arduino board and the computer is by means of a USB port connection, and the Arduino sketch loaded into the board has the ability to decode the received data from the EKG-EMG board (Fig. 16) and send it away to the Serial Port (Fig. 12).

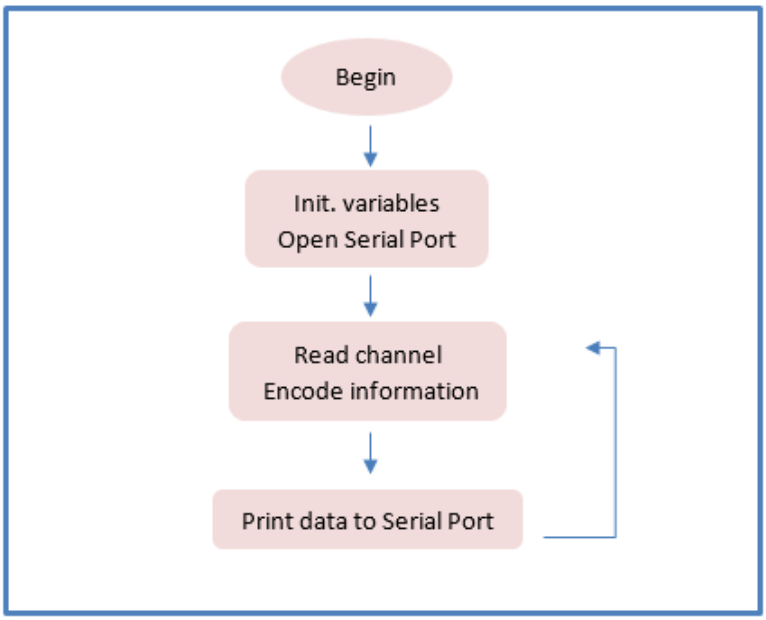

Fig. 16 Arduino flowchart analysis platform: (1) read of the current channel where information flows in and gets encoded as "A XXXX A YYYYYYY A", where XXXX correspond to values ranging from 0 to 1023 and YYYYYYY correspond to the present time in milliseconds; (2) opening of the Serial Port PC-Arduino at 57600 bauds rate, and (3) printing of the data to the Serial Port.

The Analog to Digital Converter of the Arduino board samples the ECG signal at a rate of 150 samples/s, as received by the Matlab software. The analysis platform makes sure that the signal is received in the corresponding encoded format, and then it decodes the information following real-time analysis.

3.2 Real-time analysis software packages

Three different analysis packages were developed in Matlab for analyzing electrocardiographic signals. The created algorithms implements basic ECG analysis functions for real-time beat detection and classification, and takes into account both the temporal and spectral information of the acquired signals. The overall package has the ability to:

- Identify the myocardial rhythm.
- Detect myocardial activations.
- Characterize the normal sinus rhythm of the heart.
- Detect the onset of ventricular fibrillation episodes.

Analysis of ECG signals is difficult, not only because of their physiological variability, but also because of the various types of noise that can be present (muscle noise, electrode motion, power line interface, T waves with high-frequency content similar to QRS complexes…) [39]. Although the signals are filtered on the EKG-EMG shield when acquired, in this approach, digital filters have been used to pre-filter the ECG signal and reduce the influence of all these interference sources to improve the signal-to-noise ratio (SNR).

The overall software package can be divided into three stages that are simultaneously and complementarily run:

- Myocardial rhythm detection: TOMP based.
- Fundamental frequency detection: spectral analysis.
- Ventricular fibrillation detection: Phase-Space reconstruction.

Myocardial rhythm detection

For myocardial rhythm detection, a Pan and Tompkins based algorithm was implemented in Matlab (Fig. 17).

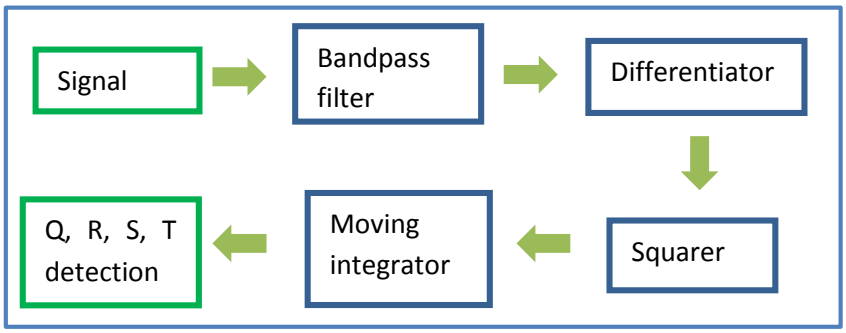

Fig. 17 Pan and Tompkins based algorithm analysis of ECG morphology features.

The bandpass step was performed in a Butterworth filter of third order: a cutoff low frequency of 5 Hz was chosen to get rid of the baseline wander, while a cutoff high frequency of 15 Hz was chosen to discard high frequency noise. Differentiation was implemented with a five-point derivative equation (2), and point by point squaring of the differentiated signal was performed (3):

$$(2) \quad y(nT) = \frac{1}{8T}[-x(nT - 2\,T) - 2x(nT\ -\ T)\ +\ 2x(nT\ +\ T)\ + x(nT + \ 2T)]$$

$$(3) \quad y\,(nT) = [x(nT)]^2$$

A difference equation (4) was used for the integration step. An appropriate value for N (number of samples in the width of the moving window) was chosen. The width of the window was set to 150ms, corresponding to around 22 samples for a sample rate of 150 samples/s (If it is too wide, the integration waveform will merge the QRS and T complexes together, and it if it is too narrow, some QRS complexes will produce several peaks in the integration waveform).

$$(4) \quad y(nT) = \frac{1}{N}\,[(x(nT) - \,(N - 1)T)\ +\ (x(nT) - \,(N - 2)T)\ + \cdots + x(nT)]$$

Fiducial marks (temporal locations) were determined from the rising edges of the waveform corresponding to QRS complexes. A minimum distance of 30 samples was considered between each R-R wave (200ms being the minimum time from a physiological point of view). Thresholds were initially set to classify current peaks as signal or noise, and they were subsequently adjusted over time depending on the wave signal.

Searchbacks for missing QRS complexes were enforced to reduce false positives in case no QRS was found for a long period of time. The minimum period of time to allow a searchback was set to 1.66 times the current RR period, and the missed QRS complex was assumed to occur at the highest peak between the threshold noise and threshold signal. The refractory period was set within 360ms of the previous QRS, and validation of real QRS complexes or their classification as abnormal predominant T waves was based on the mean slope of the signal: If the mean slope that occurs during the waveform is less than half than that of the previous QRS, it is as a T wave; otherwise it is a genuine QRS. Putative S and T peaks were found, and analyzed based on thresholding of the current mean of the signal and on slope changing: when the signal drops below the current mean value, it is analyzed whether it corresponds to a possible T peak.

Putative T peaks were detected within a 300ms time frame after S wave detection. A band limit was set between the baseline of the signal and the current S threshold value, and T waves were looked for in between: real slope change. A statistical analysis of various time intervals of interest regarding the PQRST waves of a normal electrocardiogram were also calculated during the analysis. Specifically, the mean, maximum and minimum R-R intervals were computed, alongside those corresponding to the QRS complex and the Q-T, S-T and T-T intervals.

Fundamental frequency detection

To identify the fundamental frequency of the signals, the frequency content was characterized by spectral density estimation, in particular, by estimating the power spectrum at different frequencies by means of the Welch's method.

- The signal was first split up into overlapping segments (the signal was divided into sections of length equal to a hamming window of 282 samples, with a number of 141 overlap samples), which were then windowed in the time domain.
- Then, the periodogram was calculated by computing the discrete Fourier transform, and the square magnitude of the result.
- The individual periodograms were finally time-averaged; this reduced the variance of the individual power measurements.

Ventricular fibrillation detection

A two-dimensional phase-space plot was generated by plotting the ECG signal x(t) on the X-axis, while the Hilbert Transform $\mathrm{ix_H(t)}$ of x(t) was drawn on the Y-axis.

Different electrocardiographic signals were inspected to identify a random behavior or dynamic law that could allow for differentiation of NSR and VF signals.

The method of box counting was applied to analyze the behavior of the phase trajectories. The entire phase-space diagram was represented as a grid of 40×40 bins. The bins through which at least one trajectory passed were considered as "visited boxes", and the others were considered as "non-visited" ones. The area of the space filled by the curve was computed by counting the number of bins visited by the ECG signal. A measure "d" was then computed as follows:

$$(5) \qquad d = \frac{\#\ \text{of visited bins}}{\text{total}\ \#\ \text{of bins}}$$

A threshold "d_0" was then set, and if "d" is higher than "d_0" ($d \geq d_0$), the corresponding ECG signal is classified as VF, if not, it is SR.

The different algorithms were individually tested by running the corresponding .mat functions for a variety of different signals of public databases and with ECG signals that had been previously recorded (NSR, VF, and increasing frequency stimulation). Deviations or failures were properly corrected when needed, and the final platform was initially tested by acquiring and analyzing ECG signals in real-time.

3.3 Electrocardiography waveform generator

To mimic the final system set-up with the Langendorff at the Laboratory, a waveform generator device was developed. It has the capability to generate repeating or non-repeating electronic signals, and it has been used in the testing and troubleshooting of the final ECG analysis platform. The created app has the ability to output different waveforms: from simple shapes such as sines, triangles or pulses, to any waveshape of interest. In this case, the waveform generator allows to output electrocardiographic signals, normal or irregular fibrillation beatings, with a specific frequency or rate.

The waveform generator consists of two parts: a hardware component being an Arduino Uno board, and a software component being a Matlab platform to interface with the electric board. The advantage of this type of design is that the circuit is practical and inexpensive, but fine-frequency tuning is difficult. The Arduino Uno board was used as a cheap Digital to Analog Converter (DAC) to output an analog voltage signal from a digital source by making use of the Pulse-Width Modulating (PWM) technique. It is a simple way to take advantage of an electronic board, of open-source hardware and software, and at a very low cost.

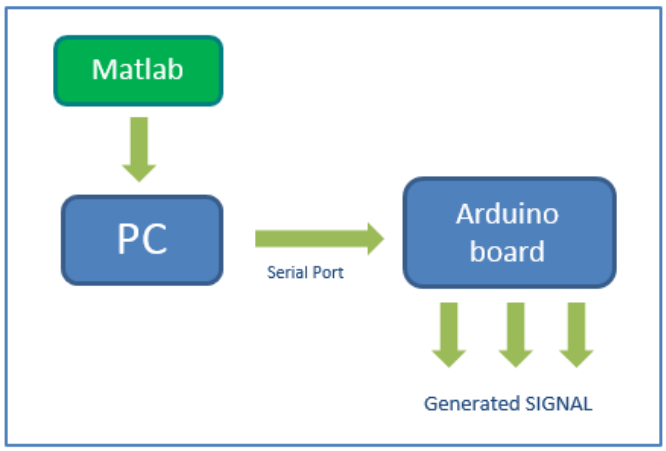

Fig. 18 Flowchart of how the electrocardiographic generator works.

The diagram in Fig. 18 shows the basic outline of how the electrocardiography generator works. The PC sends the required information to the Arduino board by means of a Serial Port (used for

communication between the PC and other devices). It is then received and decoded by the electric board, and a signal is generated.

The how-to procedure is explained in more detail below:

- The Matlab environment consists of a graphical user interface environment with built-in pre-established look-up tables corresponding to different waveshapes. The opportunity to load electrocardiographic signals of interest is paramount. The Matlab interface sends to a Serial Port arrays of values ranging from 0 to 255 and proportional to the wanted signals at specified frequencies or rates (Fig. 19A).

- The Arduino board decodes the data received from the PC (Fig. 19B) where the values, ranging from 0 to 255, are written onto a PWM pin that generates a PWM signal proportional to such values (since the Arduino board runs at 5 V, a value of 255 will correspond to such voltage).

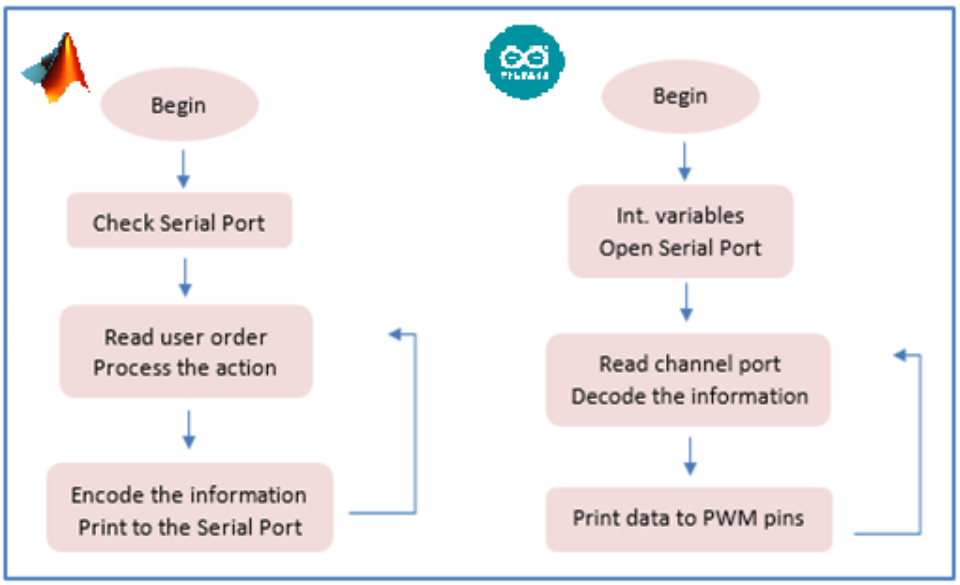

Fig. 19 A: Matlab flowchart waveform generator: (1) Checking the serial port, (2) read the user intention and process the action, (3) encode the information as "XXXX B" with XXXX corresponding to values ranging from 0 to 255, and print the information to the Serial Port at the specified frequency or rate. **B:** Arduino flowchart waveform generator: (1) open of the serial port PC-Arduino at 9600 bauds/rate, (2) read data sent from Matlab in the Serial Port, decode the data and (3) write the corresponding values ranging from 0 to 255 on the PWP pins.

- The PWM waveform must be converted into the analog voltage signal of interest, so it must go through an analog low-pass filter. A simple double RC filter (Fig. 20) was implemented with two resistors and two capacitors. The rationale behind using a double filter is that it allows reducing any noisy peaks of the output signal.

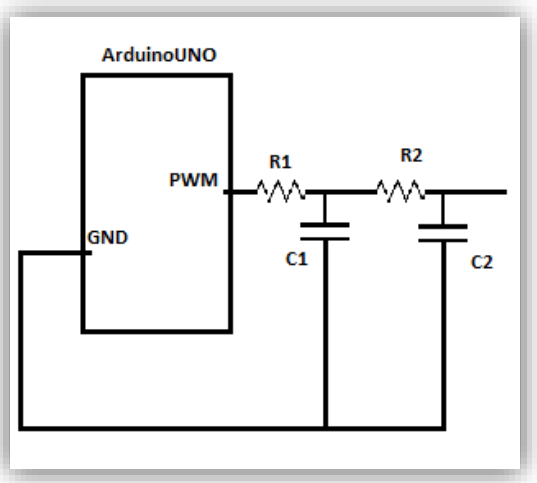

Fig. 20 Analog low-pass filter connected to Arduino UNO board.

A basic simulation of simple waveforms was first achieved, and then the code was modified to allow the output generation of electrocardiographic signals of interest.

3.3 Experimental validation

Two approaches for evaluating the performance of the registering and analysis platform were carried out: waveform simulations and ex-vivo isolated heart experiments, where the developed system was tested.

Waveform simulation

The electrocardiographic generator was tested for different signals. The simplest functionalities (sine, square, triangle signals) were checked making sure the proper signal, both in amplitude and in time, was being generated. ECG signals of sinus rhythm and with fibrillation episodes were generated from a database.

The electrocardiographic generator was run together with the real-time analysis platform. The generated signals were analyzed, and it was recorded whether or not the different functionalities of the system worked as they should: if the fibrillation episodes were detected, if the rhythm was properly computed, if the NSR morphology was distinguished, if the activation rhythm was identified, and so on.

Isolated heart experiments

For testing the developed platform, experiments mainly devoted to it were not performed. Instead, experiments that were periodically carried out at the Unit for other goals were used to minimize costs. In particular, five ex-vivo experiments with an isolated porcine heart were performed on a Langendorff bioreactor. Multi-parametric optical mapping of the heart during Langendorff was conducted as gold standard for approval of the system, measuring the transmembrane action potentials and calcium transients with high spatial resolution and without physical contact with the heart's tissue.

Preparation of the perfusate

For each Langendorff experiment two different perfusates were used: Tyrode Krebs for perfusion of the heart in the bioreactor, and Cardioplegic solution for maintaining the heart alive on its way in, with compositions according Table 1. All chemicals were obtained from Sigma-Aldrich (Dorset, UK) or Fisher Scientific Inc. (New Jersey, US).

Freshly made perfusate solutions (Tyrode 10L, Cardioplegic 4L with BDM + 2L without BDM) had been previously prepared to expedite the Langendorff experiments: the different reagents were measured in advanced according to the corresponding compositions in Table 1, dissolved in deionized water and stored as stock solutions in the freezer. The day of the experiment, the stock solutions were let to unfreeze at room temperature, the final volume was adjusted with deionized water and the pH was rectified: Tyrode's pH 7.4 at 37 ºC and Cardioplegic's pH 7.4 at 4ºC.

Tyrode solution			
	PM	[ ] (Mm)	10 L (g)
NaCl	58.44	130	76
$NaHCO_3$	84.01	24	20.2
NaH_2PO_4	138	1.2	1.7
KCl	74.56	4	3
Glucose	180.2	5.6	10.1
CaCl2	142.02	1.86	1.3
MgCl2	94.21	1	0.9
Albumin	-	-	0.4

Cardioplegic solution			
	PM	[ ] (Mm)	6 L (g)
NaCl	58.44	100	6
$NaHCO_3$	84.01	12.6	6.36
KCl	74.56	13.44	6
Glucose	180.2	280	302.76
Mannitol	182.2	34	37.14
BDM	101.11	10	4.04 (4 L)
Heparin			

Table 1 Tyrode-Krebs and Cardioplegic solution composition

The monitor equipment of the Langendorff system was arranged too, making sure the corresponding pressure pumps, flow reservoirs and thermometers were working properly before bringing the heart for the experiment.

Harvesting and perfusion of the heart

For each experiment, a minipig was taken from the Animal Facility of the Hospital, terminally anaesthetized with ketamine (25 mg/kg i.m.) and treated with heparin to avoid formation of thrombus that might obstruct the coronary arteries. The heart was isolated and surgically removed from the terminally anaesthetized porcine mammal by means of a thoracotomy procedure. The protocol had been approved by the Hospital ethics committee, and the procedure, which was performed by specialized researchers of the Unit and physicians associated with the Cardiology Department, followed animal care recommendations according to national and international legislation based on the Declaration of Helsinki regarding ethical issues of animal experimentation.

Once the heart was removed, it was placed in cold Cardioplegic solution (no BDM, 4ºC) and flushed thoroughly to remove any blood particles by contraction of the heart. Once all blood

particles were removed, the heart was cannulated through the aorta, placed in a cold Cardioplegic solution (BDM, 4 ºC) and transported to the Laboratory.

At the Laboratory, the cannulated heart was attached to the Langendorff system (Fig. 21) and perfused with the prepared Tyrode solution at 70 mmHg for its maintenance. Oxygenation of the perfusate was carried out with a mixture of 95 % O2 and 5 % CO2. The temperature was maintained at 37°C and continuously monitored together with flow rate and pressure.

An electrode catheter was placed in contact with the epicardium surface of the free wall of the left ventricle of the heart, positioned around 5mm form the lateral side of the heart.

Fig. 21 Langendorff bioreactor set-up at the Unit of Electrophysiology and Arrhythmias within the Laboratory of Bioartificial Organs and Scaffolds.

Optical Mapping

Stock solutions of voltage (di-4-ANEPPS, voltage sensitive probe TEFLabs Inc., Austin TX US) and calcium sensitive dyes (Rhod-2 AM, Ca2+ sensitive probe TEFLabs Inc., Austin TX US) had been previously prepared and stored in the freezer. A single porcine experiment requires approximately 800µL of each dye solution.

On the day of the experiment, 5mg of voltage and calcium dye probes (di-4-ANEPPS and Rhod-2 AM, respectively) were unfrozen and diluted in 2.4 ml of DMSO (2 mg/ml) from which 800µL were injected into the Tyrode solution, which was perfused through the coronary arteries for 1 to 2 minutes. Once the preparation was stabilized, and after 30 minutes in the Langendorff system, the optical mapping (Fig. 22) protocol was conducted:

Fibrillation episodes were electrically induced on the heart with a bipolar electrode (0.125mm in diameter, 1mm inter-electrode distance) located in the apex of a multi-electrode catheter. An increasing frequency pacing ranging from 4 to 20 Hz was generated with an electrical stimulator (OMLAB, Climent AM, Guillén SM). The signal used for inducing VF was a rectangular pulse (2ms wide, double intensity than that of the diastolic threshold). Stimulation was stopped once a VF episode was identified on the analysis platform. The region of the heart to image and optically

map was physically immobilized to minimize motion. Immobilization was performed only just before the images were acquired, by holding the heart between two clear Plexiglas sheets. Room light was turned off and fluorescence was excited with a green/red LED source light (CBT-90-G, peak power output 58 W, peak wavelength 524nm, Luminus Devices Billerica US), with a plano-convex lens (LA1951; focal length 25.4mm, Thorlabs New Jersey US). The emitted light was transmitted through a green/red excitation filter (D540/25X, Chroma Technology, Bellows Falls US) and recorded with an electron multiplying charge-couple device (EMCCD, Evolve-128: 128x128, 24x24 µm square pixels, 16 bit, Photometrics Tucson AZ US) with a custom emission filter (ET585/50-800/200M, Chroma Technology) connected to a data acquisition system (OMLAB, Climent AM, Guillén SM). Video images were acquired with a sampling rate of 1KHz.

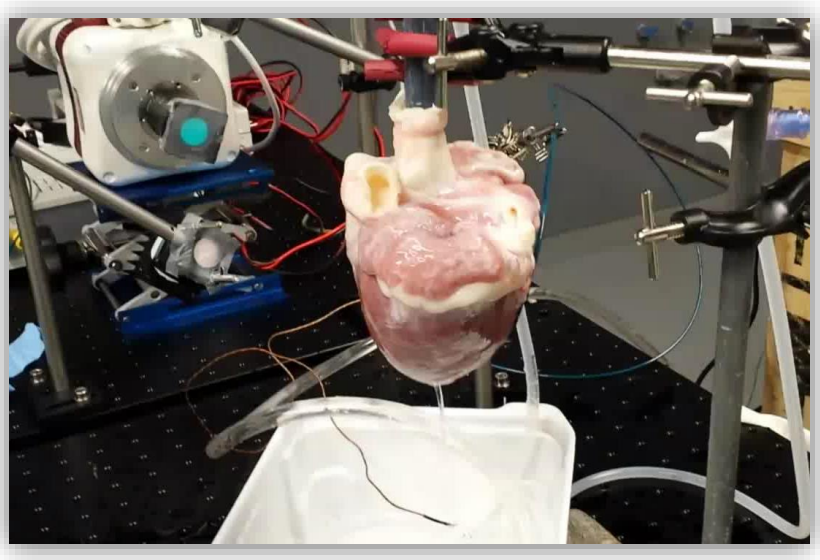

Fig. 22 Porcine heart on Langendorff bioreactor during optical mapping technique with CCD camera. Schematic illustration of the overall single-camera imaging/multiple-LED excitation system.

In this sense, the entire epicardium of the porcine heart was mapped, and optical recordings were performed providing a global view of the evolution of reentrant circuits during fibrillation. Electric signals were recorded, real-time analyzed during the optical mapping experiment and stored for further processing.

Off-line data analysis of the acquired optical mapping signals was performed with custom made modified software based on Matlab (AnalizeOM, Climent AM, Guillén SM) (Appendix III). First, files were loaded into the user-interface GUI and the region of interest for the analysis was selected. Then, signals were inverted and filtered (spatial filtering: 5 pixel kernel size, time smoothing filtering: 5 pixel kernel size) to remove noise. Finally, the power spectrum was determined (Welch periodogram, 2 second Hamming window overlap), and a Dominant Frequency (DF) map at any pixel location of the recorded activity was reconstructed to estimate local activation rates (frequency with the largest peak in the spectrum between 0.05 and 30 Hz). Phase maps of each movie were obtained by calculating the instantaneous phase of the Hilbert transformed optical recordings.

4. Expenditure

A brief summary of the expenditure expected for a project of the type is provided. The estimated costs come from the equipment and materials used, and from the human resources spent. Some costs of the materials are calculated based on the number of experiments performed. There are elements for which the unit cost is considered as the whole. Equipment is based on their depreciation in time and the total time of usage.

Materials	Unit cost (€)	€/exp.	Total €
Arduino UNO	20	----	20
Arduino Mega2560	35	----	35
EKG-EMG shield board	20	----	20 x 2units
Electric components (resistors, capacitors, cable, cable insulation…)	3	----	3
Protoboard	10	----	10
Welder tool (including tin solder wire)	15	----	15
USB cable	2	----	2 x 2units
Minipig heart (including operating room, anesthesia, physician…)	----	400	400 x5exp
Chemical reagents	----	20	20 x5exp
Fluorescent probes	350	40	40 x 5exp
			2427 €

Table 2 Materials expenditure

Equipment	Unit Cost (€)	Lifespan	€/year	Total €
Personal computer	1000	5 years	200	100 (6months)
MS Office 2010	140	1 year	140	70 (6months)
Open-source Arduino IDE	0	----	0	0
Software Matlab R2012a	250	1 year	250	125 (6 months)
Langendorff bioreactor (including the optical mapping system)	100000	10 years	10000	1000 (5exp)
				1295 €

Table 3 Equipment expenditure

Personnel	Salary (€/h)	Hours	Cost (€)
Biomedical Engineering	20	380	7600
Lab technician	15	20	300
Project coordinator	35	100	3500
			11400 €

Table 4 Personnel expenditure

The final cost estimation (Table 2, Table 3 and Table 4) for this project is of **15122 €.**

5. Results

The outcomes of this project are presented in this section. The developed registering and analysis system will be shown, along with examples of how the platform would be functioning in real-time. Results obtained with the developed electrocardiographic waveform generator will be disclosed, and the aftermath validation strategy regarding waveform simulation and isolated heart experiments will be analyzed.

5.1 Acquisition and registering system

A brief understanding of the final assembly and functioning of the developed real-time acquisition and registering system is shown.

The basic circuitry of the system is depicted in Fig. 23. As shown, a catheter is connected through the jack connection to an EKG-EMG board that piggybacks on top of an Arduino Mega2560 connected to a PC by an USB cable.

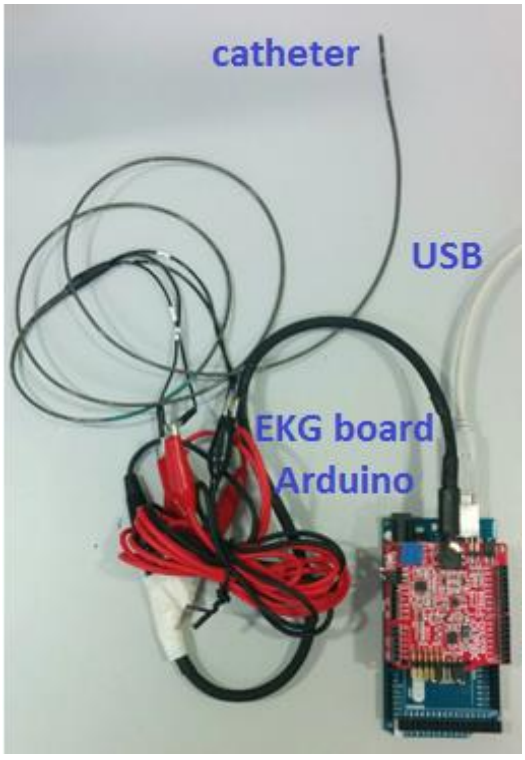

Fig. 23 Registering and analysis platform set-up. A catheter is connected through the jack input to an EKG-EMG board that piggybacks on top of an Arduino Megea256 connected to a PC.

The software interface (see Appendix II) of the developed system is shown in Fig. 24, together with an example of a real-time acquired electrogram at 141 samples/s. According to the system, the sample corresponds to a normal sinus rhythm as no VF warning appears. Myocardial

activation is shown to have a fundamental frequency of 1.27 Hz based on spectral analysis. This correlates with the identification of the myocardial rhythm at 78 beats/min.

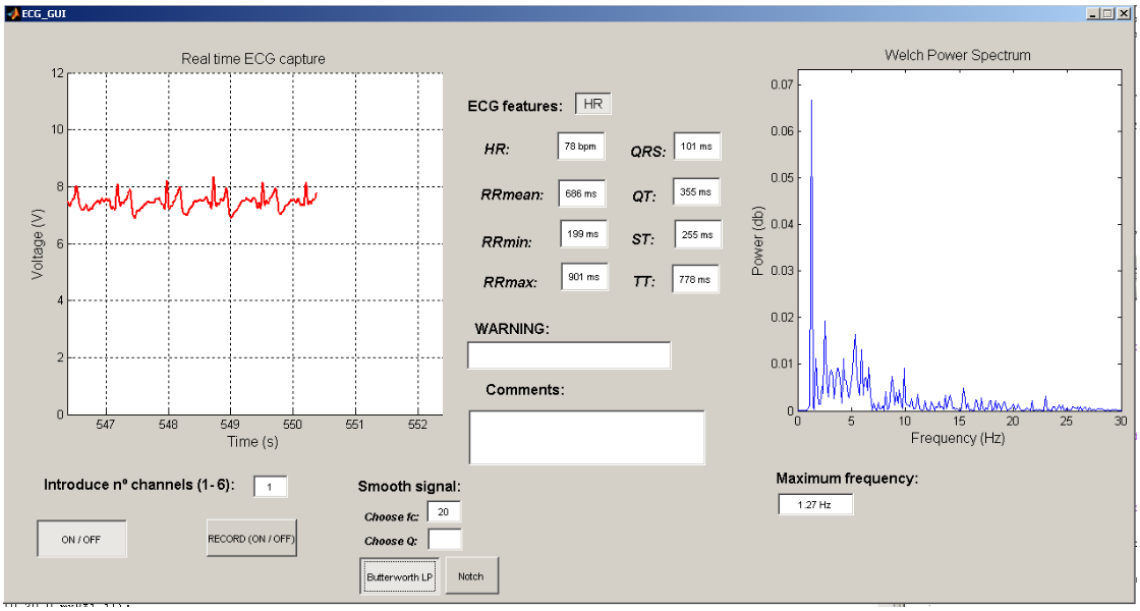

Fig. 24 Software interface of the registering and analysis platform. An example of a real-time acquired electrogram at 141 samples/s is shown: normal sinus rhythm, fundamental frequency of 1.27 Hz, myocardial rhythm of 78 beats/min.

5.2 Real-time analysis software packages

The functioning of how the system would be working in real time is illustrated here. In the following sections, representative examples regarding each one of the software blocks are shown.

Myocardial rhythm detection

About 6 seconds of a raw human ECG signal acquired with the developed platform at a sampling rate of 141 samples/s is illustrated in Fig. 25. The signal shows the trend of a normal sinus rhythm electrocardiogram, with the characteristic P, Q, R, S and T waves easily observed.

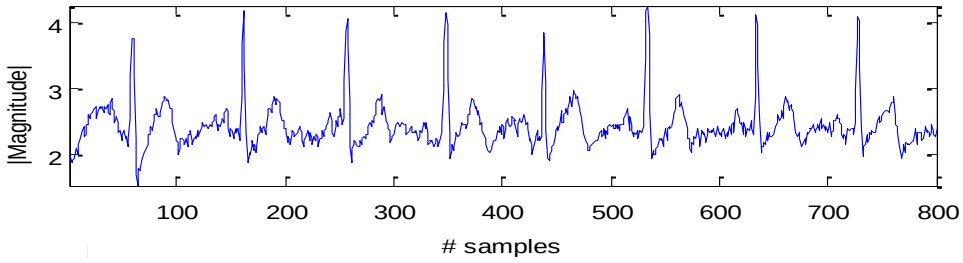

Fig. 25 Raw ECG signal acquired at a sampling rate of 141 samples/s with the developed platform.

The signal had been filtered and analyzed with the TOMP based algorithm. In Fig. 26, a smoothed ECG signal after being bandpassed between the frequency range of 5 and 20 Hz to enhance detection of the QRS complexes is drawn.

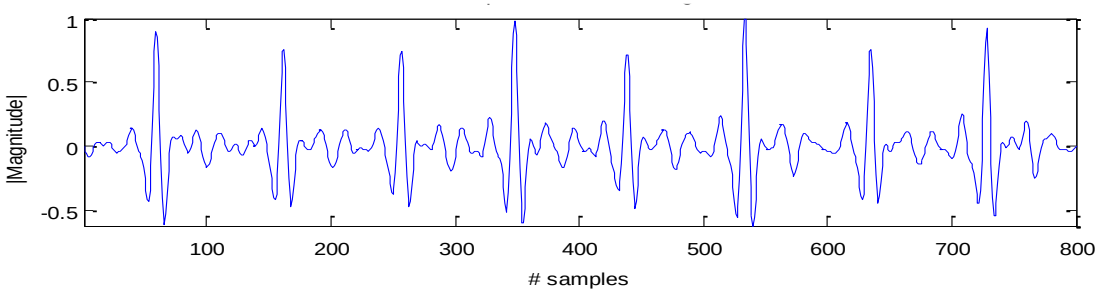

Fig. 26 Bandpassed ECG signal between 5-20 Hz

A squared ECG signal as a sort of pulse trains for easier detection of the QRS complexes within the signal appears in Fig. 27.

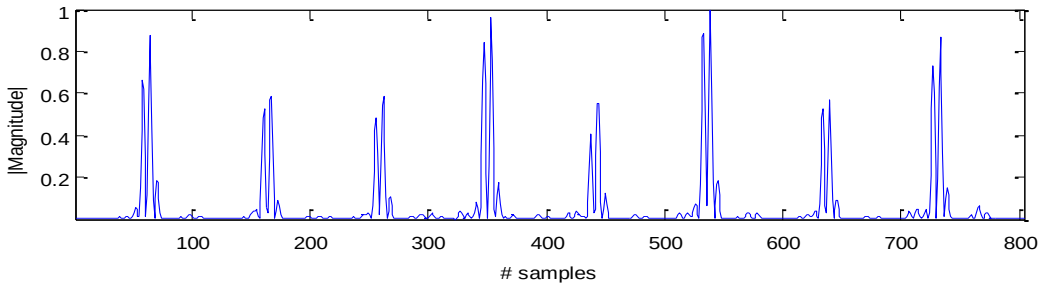

Fig. 27 Squared ECG signal with enhanced QRS complexes

In Fig. 28, QRS complex detection on a moving average (MVI) filtered ECG signal is depicted. Pulse trains are easily identifiable after the squaring step, where the ups and downs of the signal have translated into clear pulses of width equal to the QRS time interval. Threshold levels have also been plotted (black corresponding to noise level, green corresponding to the adaptive threshold level and magenta corresponding to the signal level).

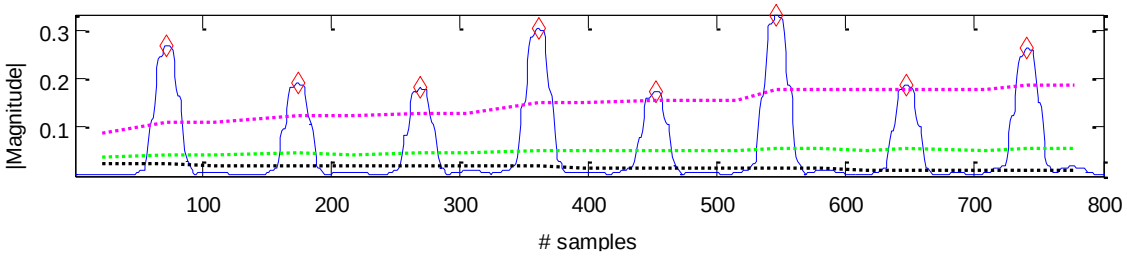

Fig. 28 R-R peak detection on a moving average filtered ECG signal. Pulse trains are easily identified (red diamonds) corresponding to the QRS complex. Threshold levels (black corresponding to noise level, green corresponding to the adaptive threshold level and magenta corresponding to the signal level).

Detection of the Q, R, S and T waves after filtering, smoothing and pre-processing the ECG signal of Fig. 25 are shown in Fig. 29.

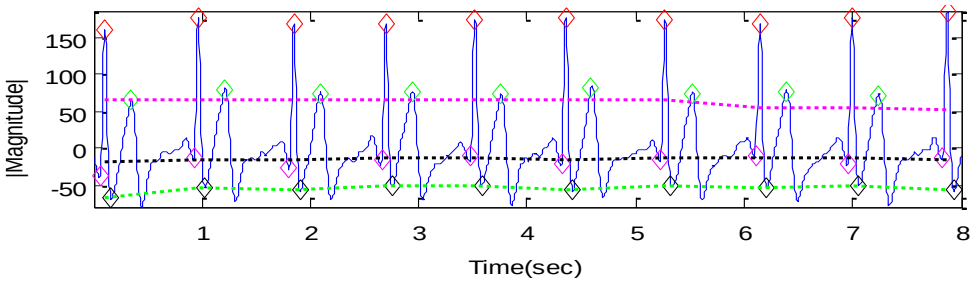

Fig. 29 Q,R,S and T detection after filtering, smoothing and pre-processing of a raw electrocardiographic signal. Legend: red diamond corresponding to R peaks, green diamonds corresponding to T peaks, magenta diamonds corresponding to Q peaks and black diamonds corresponding to S peaks. Threshold levels: magenta corresponding to T waves, black corresponding to Q waves and green corresponding to S waves.

Detection of myocardial activation for identification of the rhythm is shown in Fig. 30. As it can be appreciated, the straight line pulses go through just the middle of the aforementioned QRS complexes.

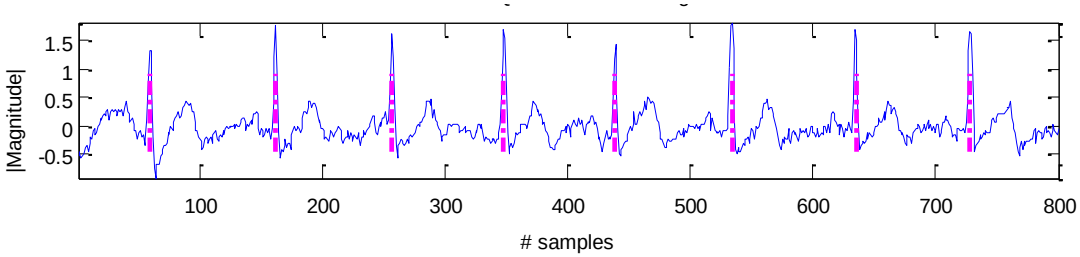

Fig. 30 Myocardial activation shown as line pulses on the corresponding raw ECG signal.

Ventricular fibrillation detection

In this section, representative examples regarding onset detection of ventricular fibrillation by means of the phase-space reconstruction algorithm are shown.

Two completely different types of signals had been analyzed: one corresponding to an irregular random and chaotic behavior, typical of VF signals, and another one corresponding to a regular and periodic behavior of an ECG of normal sinus rhythm.

Results of the comparison are depicted in Fig. 31, where their typical two-dimensional trajectories have been drawn based on the Hilbert Transform and according to the phase-space reconstruction delay method. Evidently, VF and normal ECG signal trajectories exhibit totally different behaviors. The display on the X-Y space follows a characteristic trend: for the case of the VF signal (A), the phase-space diagram fills the plane producing a curve in the space in a chaotic and irregular way, distributed all over the entire area. However, phase-space plots of NSR ECG signals (B) present circle-like curves at more restricted and smaller locations within the diagram. The more rhythmic and regularity behaviors of normal ECGs can be seen in their trajectory, which behave more similar to the trajectory of a deterministic system. Based on the differences on their state space features, it would be expected that VF and NSR signals could be differentiated and classified.

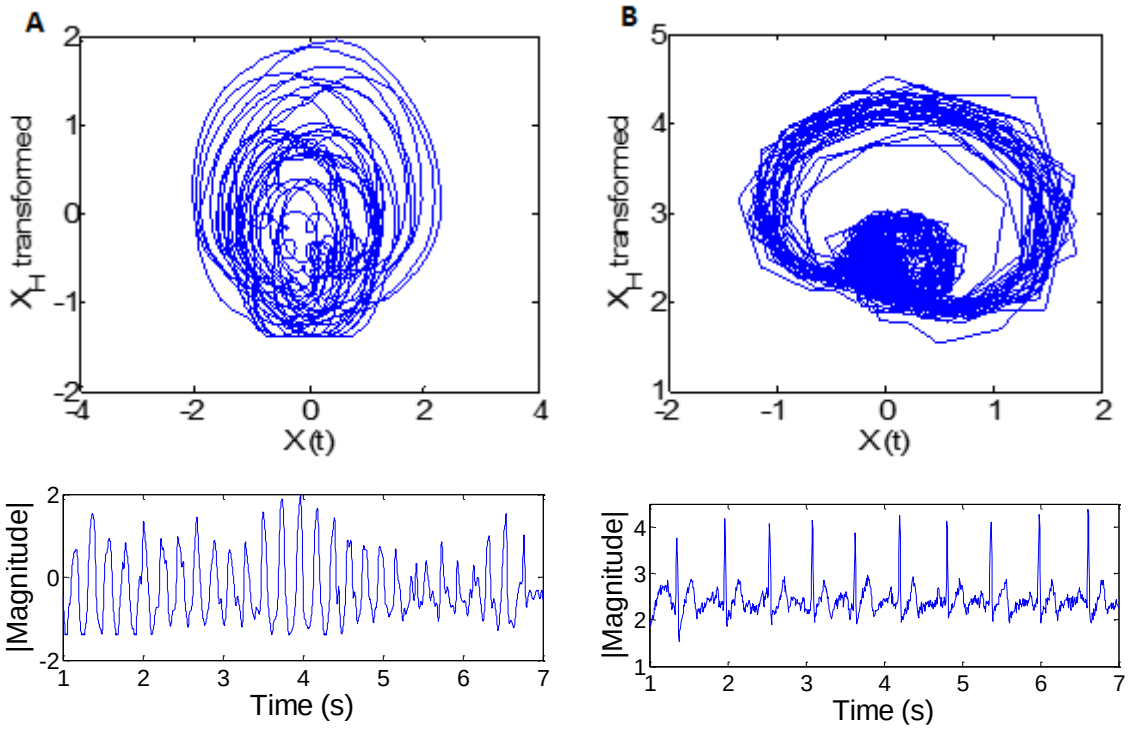

Fig. 31 Two-dimensional trajectories of a VF signal (**A**) and of a normal ECG signal (**B**) drawn in the phase-space X-Y, with their corresponding electrograms below. Signals of a more random and chaotic behavior fill the entire plane in a more irregular way (**A**), while those of a more periodic regular behavior present circle-like curves at more restricted and smaller locations within the diagram (**B**).

Phase-space images of the aforementioned two-dimensional trajectory behaviors are depicted in Fig. 32, where the state space containing the trajectories is portioned into a 40 X 40 grid.

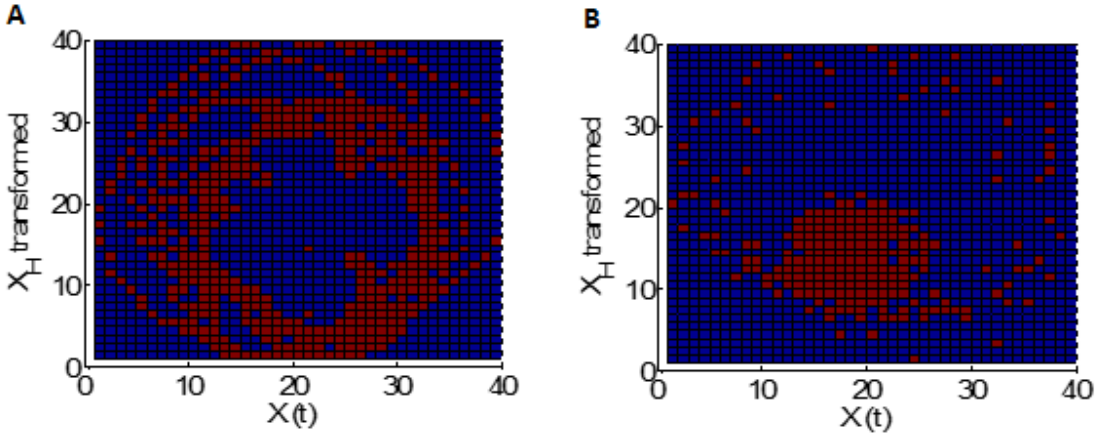

Fig. 32 Phase-space image reconstruction of 2D-trajectories of a VF signal (**A**) and a normal ECG signal (**B**). The phase-space is portioned into a 40 X 40 grid to allow extracting informative features and estimate the degree of complexity or chaotic dimension of each signal

Taking the average of each column within the grid, a curve characterizing the distribution of points in the phase-space can be obtained. An example of such curve, for a normal sinus rhythm and for a ventricular fibrillation signal type, is depicted in Fig. 33, revealing their discrimination capacities. It is clear that the area under the curve can be used to distinguish between ECG signals. As seen for VF signals, the area under the curve is more distributed throughout the

whole space, and its total percentage is higher than in the case of the NSR signal type, which is more regionally localized.

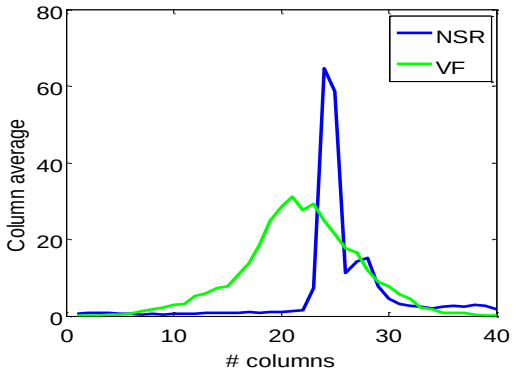

Fig. 33 Matrix column average distribution for VF (green) and SNR (blue) signal types.

A three-dimensional glimpse of the phase-space reconstruction regarding Fig. 32 is illustrated in Fig. 34. As seen for the case of the VF signal (A), the entire diagram is uniformly filled with more or less peaks of the same height, while for the case of an ECG signal of normal sinus rhythm (B), peaks of similar length seem to concentrate in a more restricted area of the diagram.

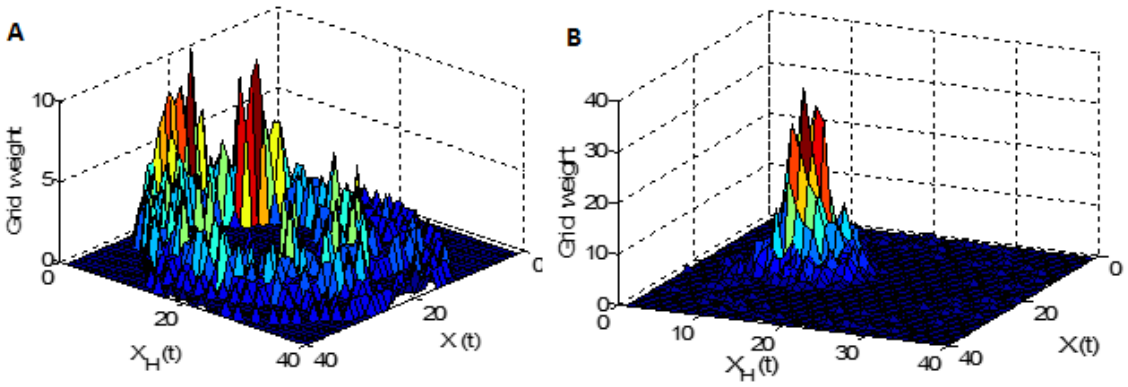

Fig. 34 3D phase-space reconstruction of the trajectories of a VF signal (**A**) and of a normal SR ECG signal (**B**). The entire diagram is uniformly filled with peaks of the same height for the VF signal, while for the case of the NSR signal, peaks seem to concentrate in amore restricted area of the diagram.

Fundamental frequency detection

Examples of frequency spectrums regarding detection of the fundamental frequency of the signals are presented.

Frequency spectrums during frequency pacing stimulation at 600 and 150ms (A, B respectively) and during ventricular fibrillation episodes (C, D) are depicted in Fig. 35. As it can be seen, detection of the fundamental frequency correlates with the rate of frequency pacing (A, B), and ventricular fibrillation episodes (C, D) exhibit higher frequency content when compared to normal sinus rhythms.

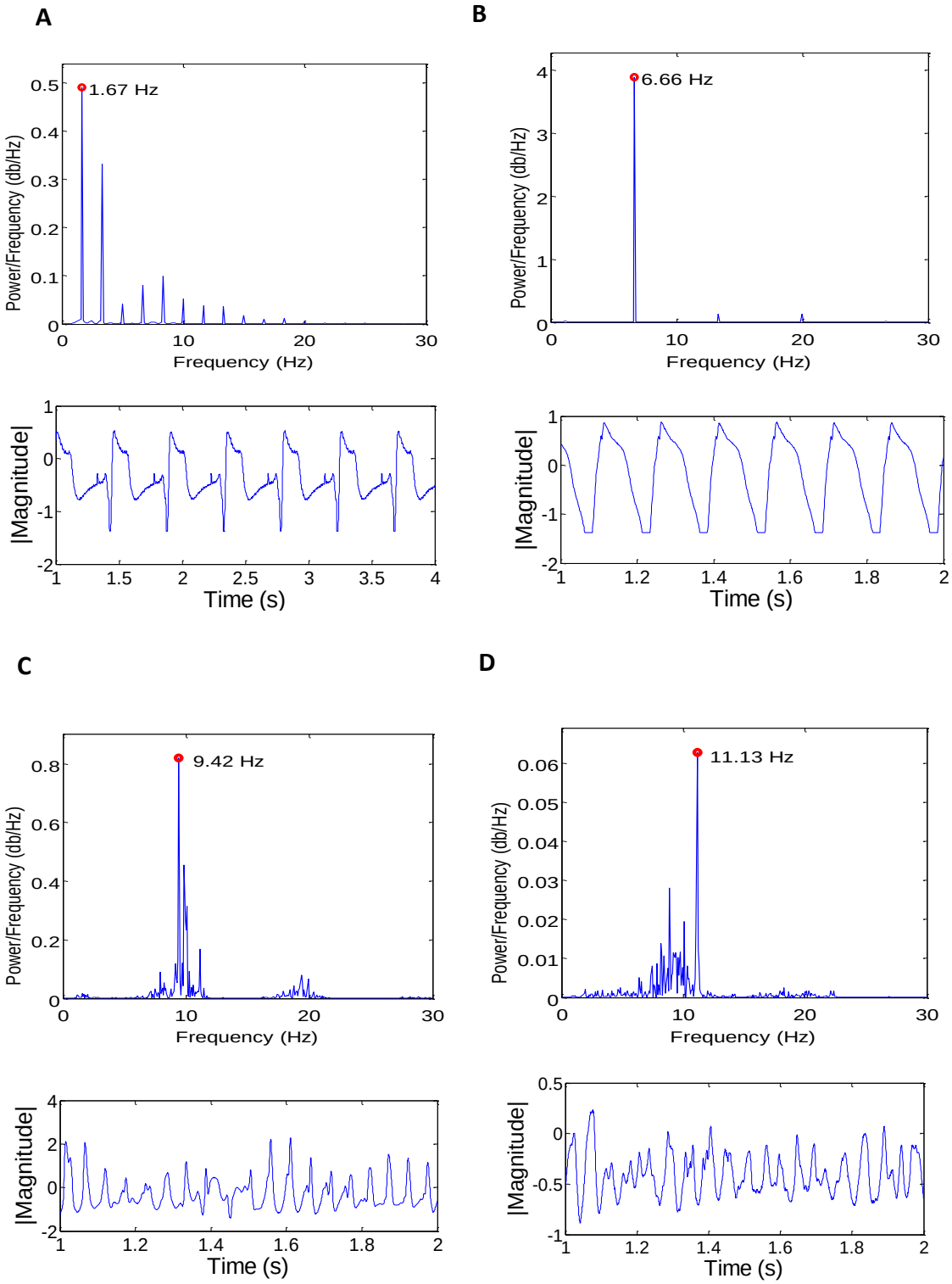

Fig. 35 Frequency spectrum of a NSR during stimulation at increasing pacings: 600 and 150ms respectively (A, B) until ventricular fibrillation was induced (C, D). Corresponding electrograms are shown below.

5.3 Electrocardiographic waveform generator

The set-up of the developed electrocardiographic waveform simulator is presented, along with its interface.

The final assembly of the simulator is described in Fig. 36: an Arduino UNO board connected to a PC by means of an USB cable. The PWM output signal goes through a second order filter in a protoboard where conversion to an analog signal would take place.

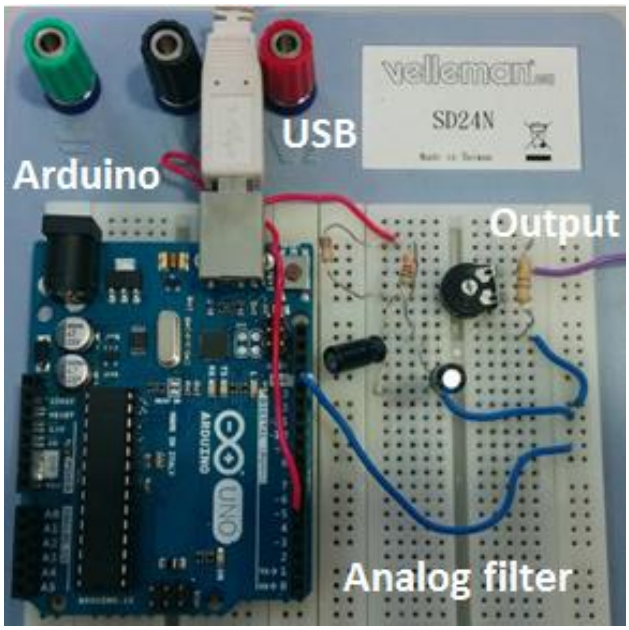

Fig. 36 Set-up of the electrocardiographic waveform simulator: an Arduino UNO board is connected to a PC by means of an USB cable. The PWM output signal goes through a second order filter in a protoboard where conversion would take place.

An example of the user interface is shown in Fig. 37 (see Appendix I):

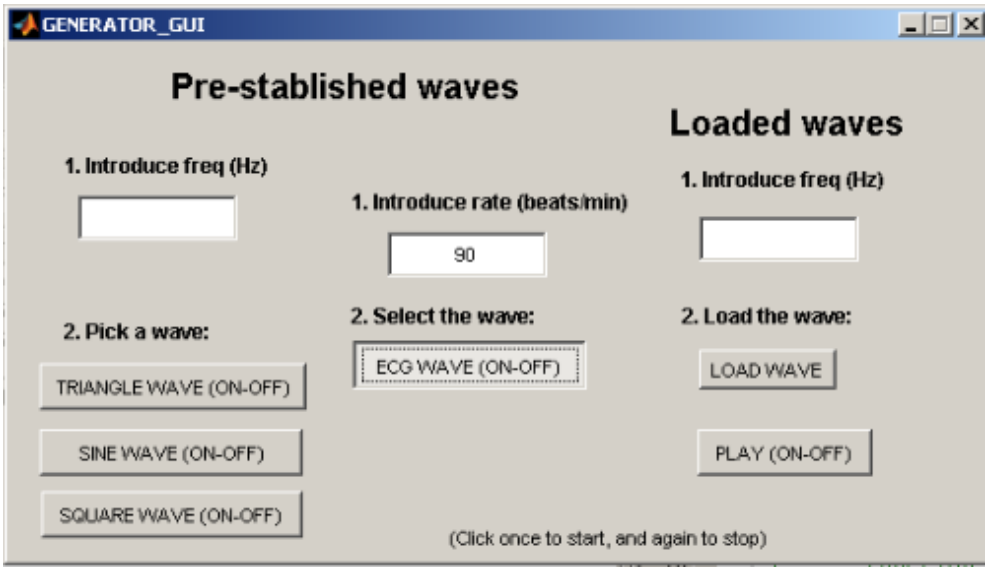

Fig. 37 Interface of the electrocardiographic waveform simulator.

5.4 Experimental validation

In this passage, results obtained from the experimental evaluation of the developed real-time registering and acquisition system are presented. Two subdivisions are made: results obtained from the electrocardiographic waveform simulator, and results obtained during ex-vivo isolated heart experiments.

Waveform simulation

This section demonstrates the functioning of the developed electrocardiographic waveform generator for testing the real-time registering and analysis platform.

The assembly of the developed electrocardiographic waveform simulator together with the real-time registering and analysis platform is shown in Fig. 38. The connection between the two is by means of a jack input connector.

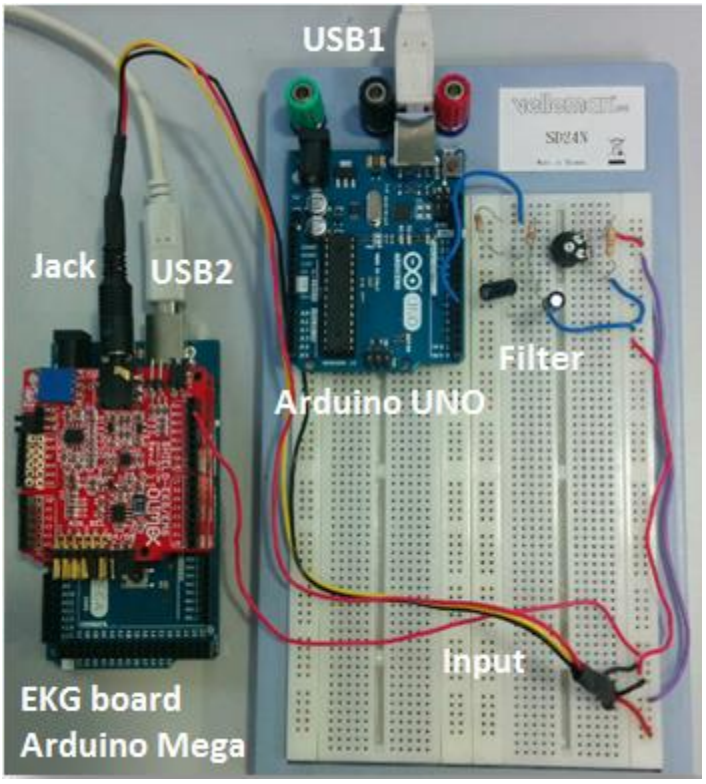

Fig. 38 Assembly of the electrocardiographic waveform simulator together with the developed real-time registering and analysis platform during experimental validation.

A sinusoidal and a triangle signal generated with the waveform simulator to test the early basic functioning of the real-time registering and analysis platform is represented in Fig. 39. The sinusoidal signal was generated at 1Hz, while the triangle signal was generated at 4Hz. As shown, signals are faithfully registered by the system and detection of the fundamental frequency is quite accurate.

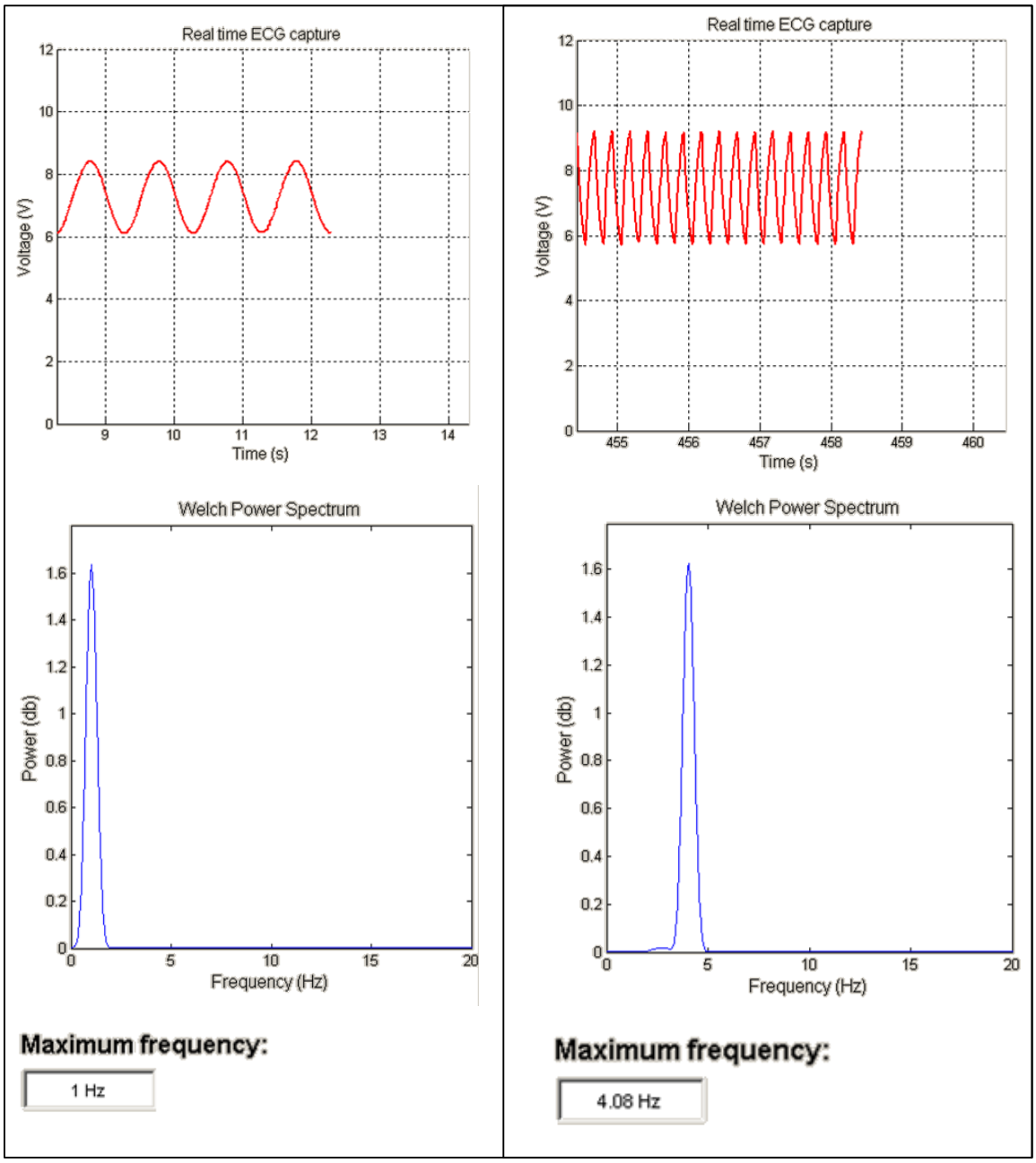

Fig. 39 Sinusoidal and triangle signal generated with the waveform generating platform during earlier testings.

More complex signals are shown in Fig. 40. A normal SR ECG signal is illustrated on the left side, generated at 2Hz, with its frequency spectrum depicted below. Fundamental frequency is detected at 2.17Hz. On the right side, a VF signal generated at 8.5 Hz is displayed in the range, being 8.75Hz its detected fundamental frequency. As it can be seen, only slight variations are produced.

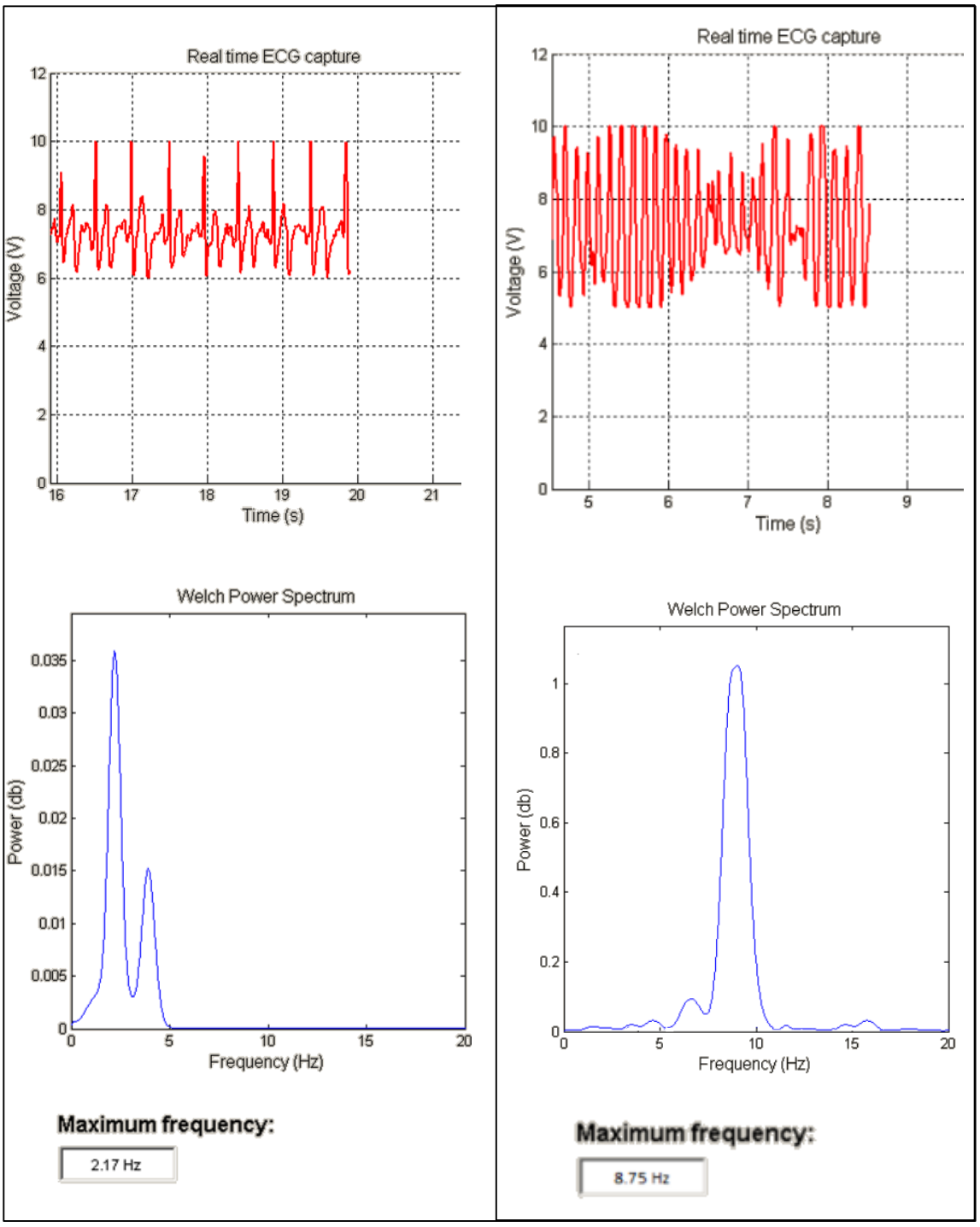

Fig. 40 Normal SR ECG signal generated at 2Hz is shown above, while a VF signal is displayed at the bottom.

Isolated heart experiments

Some examples regarding evaluation of the real-time registering and analysis system during experiments carried out with isolated porcine hearts in a Langendorff bioreactor are provided. Comparisons with off-line analysis of their corresponding optical recordings (gold standard) are described.

Optical mapping of the heart was performed during Langendorff (Fig. 41), with its surface being irradiated by light sources (Fig. 42). As it can be seen, lights were off to decrease the probability of photobleaching during the experiments and to allow selected wavelengths of light to reach the detector.

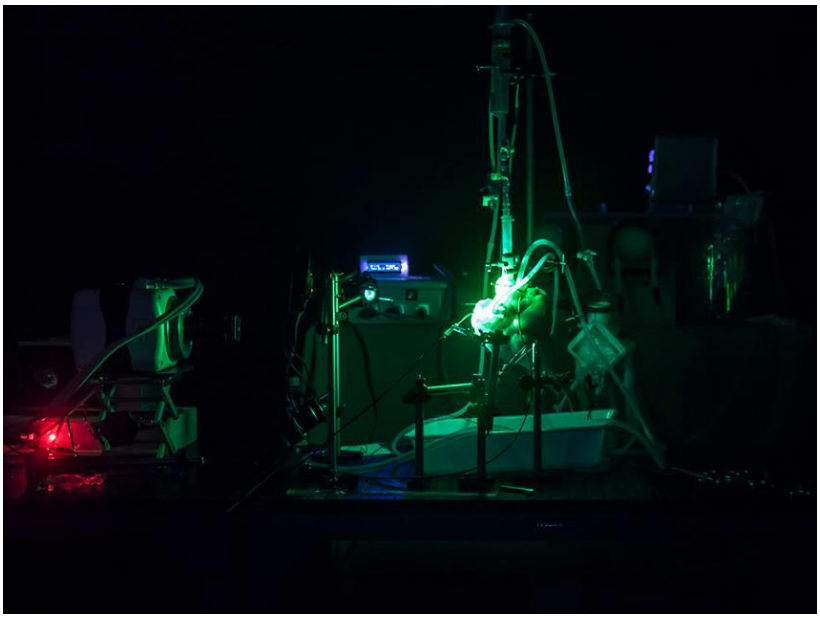

Fig. 41 Optical mapping during a Langendorff experiment of an isolated porcine heat model.

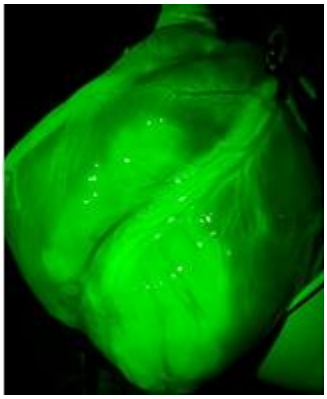

Fig. 42 Heart surface being irradiated by green light.

The sequence in Fig. 43 portrays how the electrical activity of the myocardium flows through the heart towards the apex, with a stimulating catheter placed on the bottom. Some voltage signals are also plotted, corresponding to the depolarization and repolarization of the cardiomyocytes (Fig. 44). An isochronal map of the flow stimulation is also shown in Fig. 45.

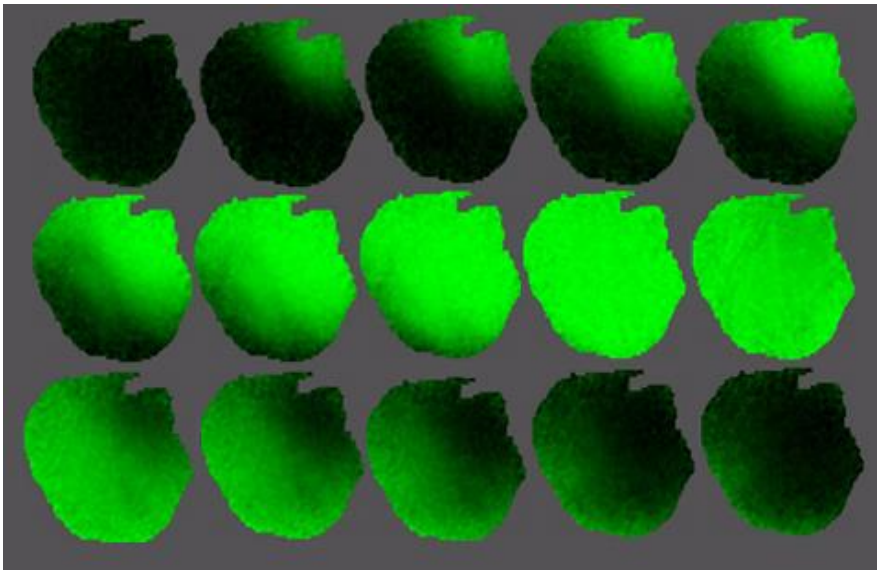

Fig. 43 Electrical stimulation flowing from the top to the apex during optical mapping. Depolarization and repolarization is shown.

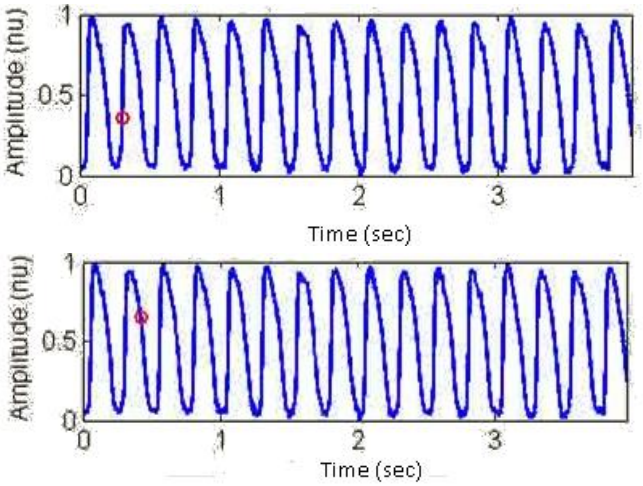

Fig. 44 Depolarization and repolarization of the heart's tissue during optical mapping.

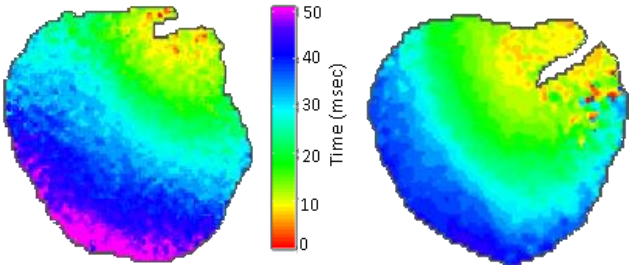

Fig. 45 Isochronal map of the heart tissue where it can be seen how the electrical impulse flows through time.

Isochronal maps are the most common means to depict an activation pattern. In this case, a normal pattern is described, with no re-entrant activations. Since isochrones connect points of equal activation time, it inadvertently suggests conduction time.

Results obtained with the developed registering and analysis platform during frequency stimulation of the heart at 600 and 450ms are shown respectively in Fig. 46 and Fig. 47. Dominant Frequency (DF) maps and Welch's power spectrums (highlighting highest frequency within DF map) obtained from their corresponding optical recordings (see Appendix III) are represented too. No ventricular fibrillation episodes were registered.

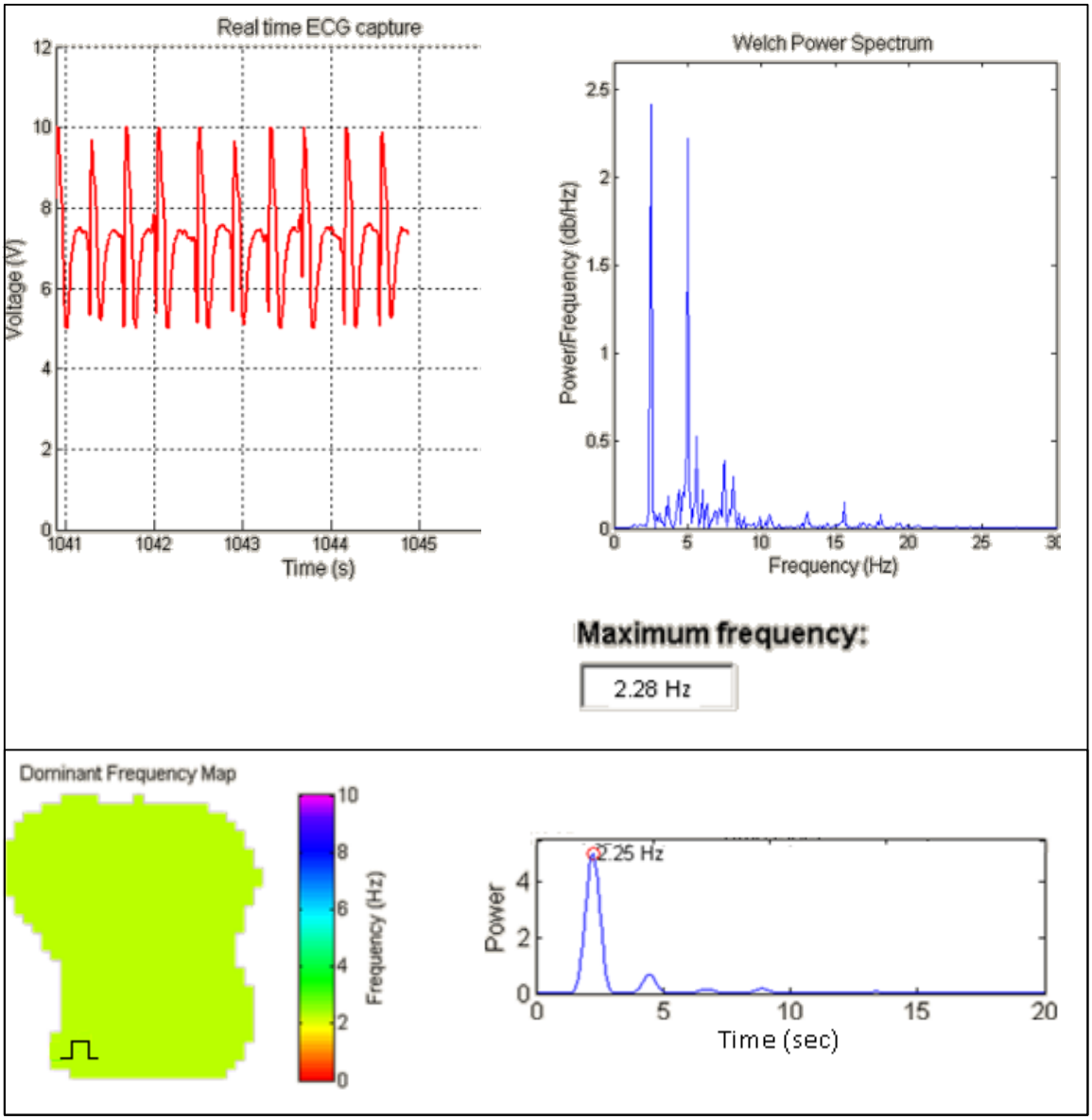

Fig. 46 Comparison between results obtained from the real-time analysis platform and from off-line optical recordings. Stimulation of the heart surface at 440ms (2.27 Hz). The black dotted represents location of stimulation catheter.

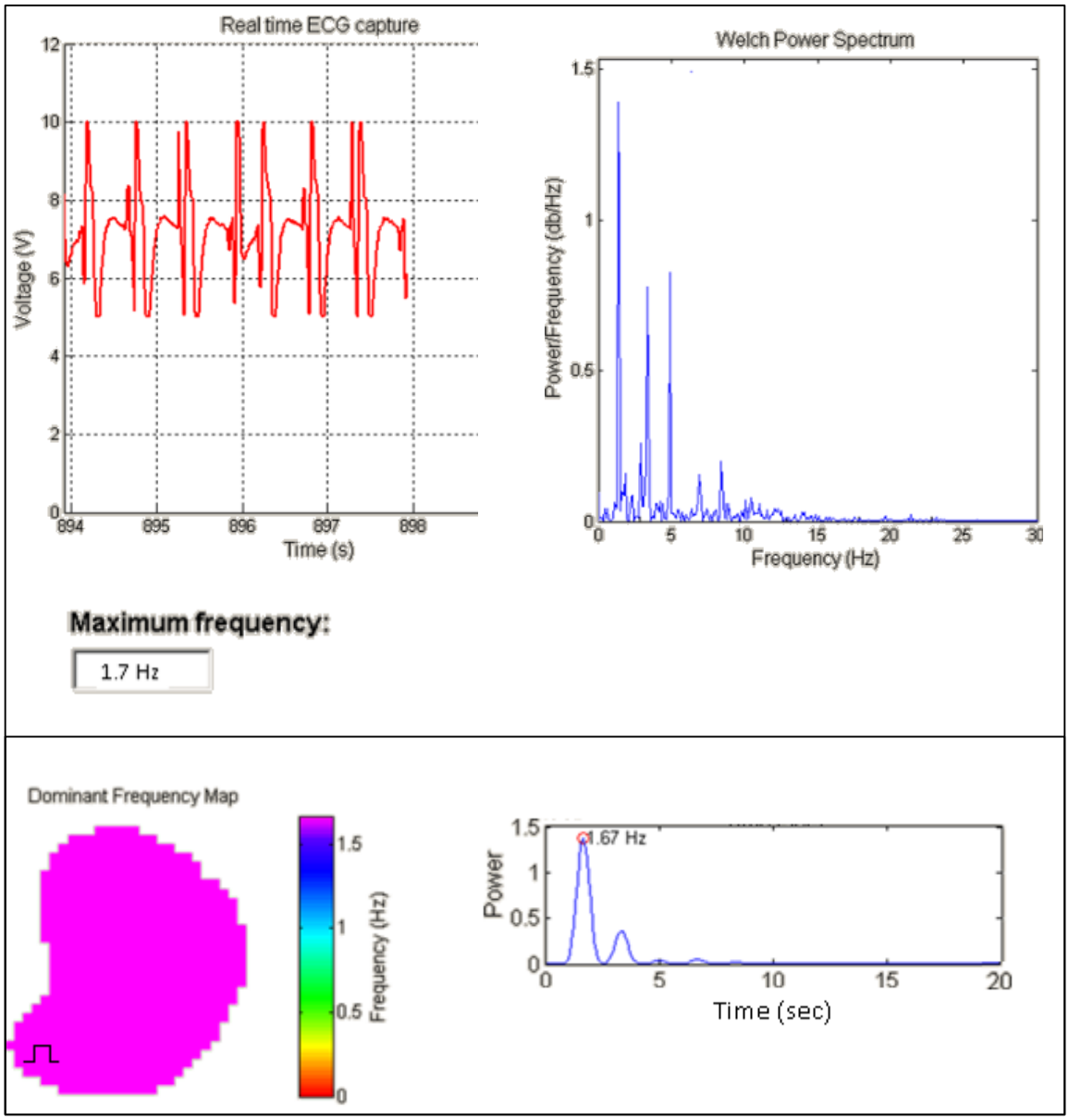

Fig. 47 Comparison between results obtained from the real-time analysis platform and from off-line optical recordings. Stimulation of the heart surface at 600ms (1.66Hz). The black dotted represents location of the stimulation catheter.

As shown in these two cases in which the surface of the heart was being stimulated at a constant rate, the DF maps obtained are uniform. For both cases, the frequency along the whole heart surface is the same, and it matches well the one detected by the developed system.

Two examples regarding comparison of results once ventricular fibrillation episodes had been induced are shown in Fig. 48 and Fig. 49. The white dotted square in the DF map represents the location of the heart surface where the registering electrode for the real-time analysis system had been positioned.

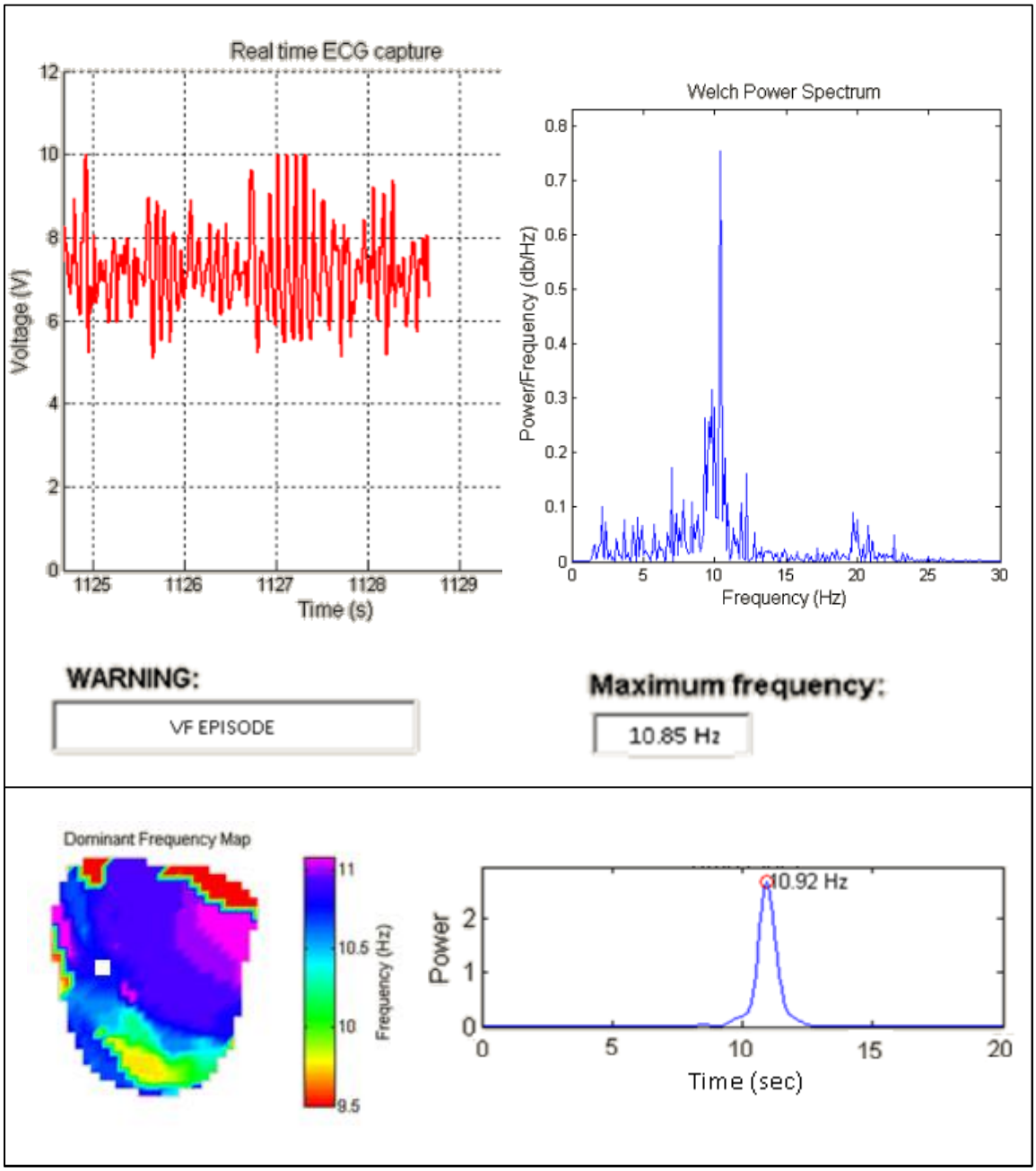

Fig. 48 Ventricular fibrillation episode A: comparison between results obtained from the real-time analysis platform and from off-line analysis of optical recordings. The white dotted square in the DF map represents the location of the surface where the registering electrode had been positioned.

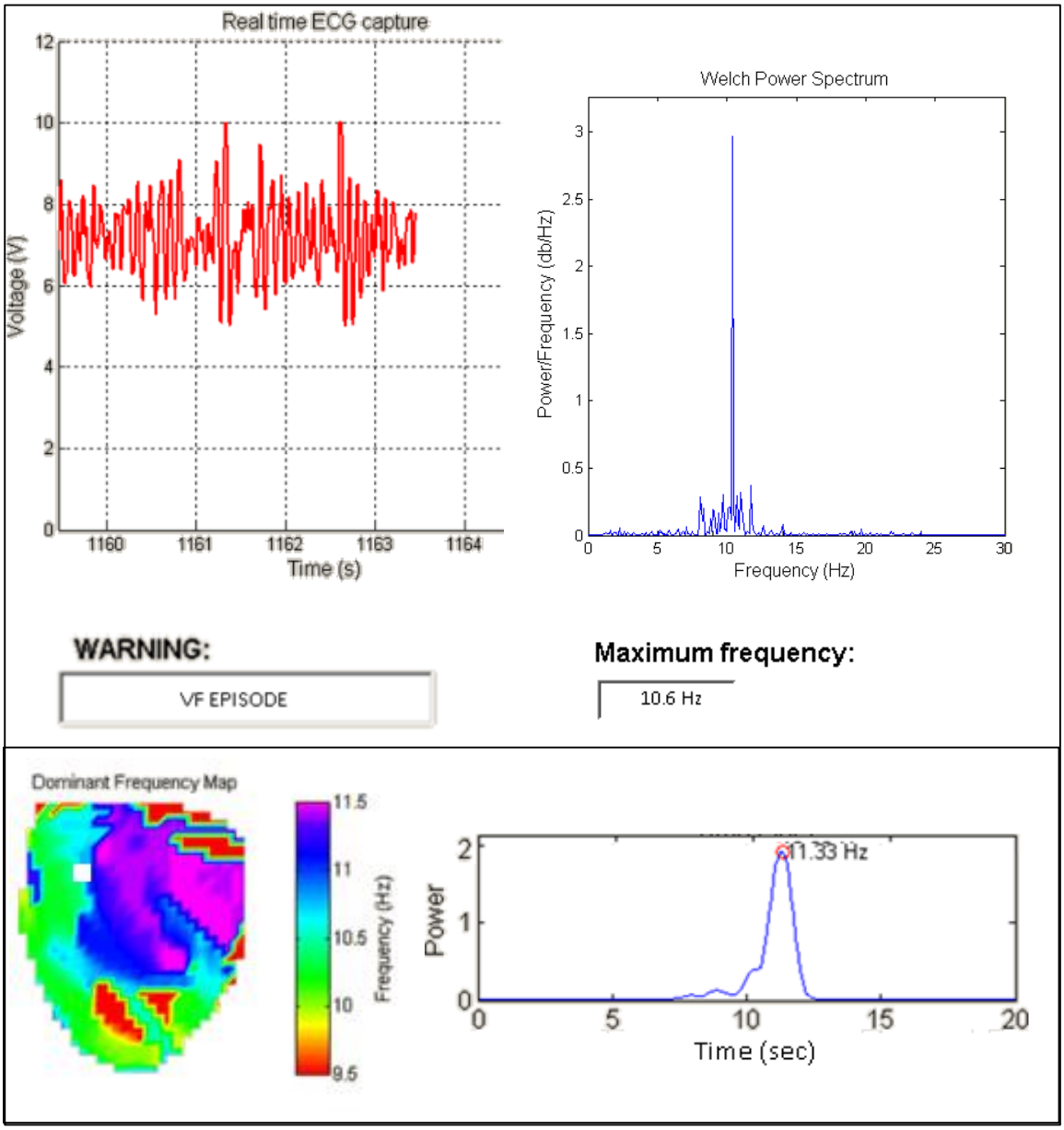

Fig. 49 Ventricular fibrillation episode B: comparison between results obtained from the real-time analysis platform and from off-line analysis of optical recordings. The white dotted square in the DF map represents the location of the surface where the registering electrode had been positioned.

In these two cases, ventricular fibrillation was already induced, and it was detected by the developed platform. Also, a convergence of many different frequencies can be seen in the DF maps, caused by the chaotic and random behavior of the signal. The fundamental frequency detected by the spectral analysis matched the corresponding region of the DF map where the registering catheter had been placed. The power spectrum obtained from the off-line analysis of the optical recording showed a maximum frequency within the DF map that did not correlate with the calculated frequency by the developed platform: the optical system maps the activity of the whole surface of the heart while electrodes only registers activity where they are placed.

6. Discussion

6.1 Main contributions

This project presents a real-time registering and analysis platform for quantification of electrophysiological signals. The system, with a low computation overhead, is aimed to be used in the context of isolated heart models, integrated as an add-on component within the elements of a Langendorff bioreactor.

Results obtained with the real-time registering and analysis platform were coherent, the random behaviors of the signals due to desynchronization phenomena of the heart tissue were detected allowing to characterize ventricular fibrillation events and differentiate them from sinus rhythm episodes. Electrical signals registered with the developed platform were in accordance with dominant frequency maps obtained from the off-line analysis of the corresponding optical recordings, showing reproducible results.

The designed application would help researchers of the Unit of Electrophysiology and Arrhythmias of the Laboratory of Scaffolds and Bioartificial Organs to quantify the complexity of electrocardiographic signals during specific therapeutic treatments under research and to help mitigate the unknowns of the onset and perpetuation mechanisms of ventricular fibrillation. This way, an objective criteria on the effect of different pharmacological antiarrhythmic drugs in an ex-vivo isolated heart model to which different arrhythmias could be induced, would allow them to determine the most appropriate solution. It is indeed an adaptable system that covers the basic current needs of the researchers of the Laboratory in an adequate and accessible way to everyone. But of paramount importance is the versatility of the platform, since it would allow incorporating different signal processing techniques depending on the needs of the current project, updating the system at any time with multiple resource-settings.

6.2 Other approaches

Optical mapping of the heart is generally used as the gold standard for quantification of the activation patterns during fibrillation, but the problem lies in the fact that analyses must be done off-line after experimentation [30]: such technique does not allow quantifying the complexity in real-time. Other than that, there exists few commercial software packages [55] available to real-time process the data collected from isolated heart experiments, however, they are not adaptable to the exact application or need that the researchers might require.

In this sense, an easily customizable computer application, which includes an intuitive graphical user interface, was developed. The system is very useful to monitor the progression of the heart functioning during Langendorff experiments, and for the reproducibility of the studies. In addition, one of the main advantages is the versatility to introduce novel analysis methods in the future.

6.3 Clinical applications

An automated method for real-time quantification of the complexity of electrocardiographic signals has several potential applications. As mentioned, it could be used to quantify the effects induced by different potential antiarrhythmic drug candidates or maneuvers that may alter the electrophysiological properties of the myocardial tissue [56–58]. In addition, it could provide an insight into differences among areas of the epicardial tissue [59].

The developed application presents an efficient and versatile way to objectify the analysis of fibrillation mechanisms, and given that it automates the classification process, it greatly reduces the amount of time needed to carry out the task, favoring productivity. Moreover, the proposed methodology has the advantage that it can migrate to other recording technologies, for instance using multi-electrodes with different configurations or with more registering points.

6.4 Limitations

Ventricular fibrillation takes place in a volume and it is, therefore, a three-dimensional process. However, the proposed methodology to quantify the complexity of electrocardiographic signals is based on recording the electrical activity between two points within a two-dimensional surface that does not represent the total epicardium. Although this methodology has proven useful to study variations in complexity induced by electrophysiological modifications, no precise conclusions can be drawn from the fibrillatory process beyond the onset of the full mechanism.

More accurate registration systems employ up to 80 needles equipped with several recording points that are introduced into the myocardium for recording the electrical activity of the heart in three dimensions [60], but these proceedings have the risk of damaging the cardiac tissue, modifying the properties of the myocardium. In any case, the proposed methodology of the developed platform can be adapted to different configurations of recording electrodes and points so that more than one endocardial/epicardial electrogram can be quantified.

6.5 Future work

In view of the limitations, some interesting lines to improve the platform could be developed. Future work will be mainly directed to increase the sensitivity and accuracy of the proposed algorithms to satisfy the needs of the Unit, and to incorporate other relevant aspects for detection and analysis in the decision system: heart rate variability (HRV) parameters, point-care plots, non-linear and complexity measures or time-frequency distributions.

The phase-space reconstruction algorithm for detection of ventricular fibrillation could be further expanded to characterize ventricular tachycardia by increasing its sensitivity for arrhythmia detection and identification of morphological changes in the ECG [52,61]. Indeed, the ability to identify and study the different organizational behaviors of phase distribution during arrhythmias could lead to a better characterization of arrhythmias in humans and provide mechanistic strategies in modulating cardiac fibrillation [48]. In addition, the phase-space

reconstruction algorithm could be used for detecting some heart diseases that may display better in the state space, but it could also happen that other diseases are rather difficult to recognize in that representation [52].

Detection of the fundamental frequency of the signal could be improved, and analysis of the ECG features and detection of the heart rhythm could be proposed instead by an approach based on wavelet analysis operating both in the frequency and time domains. This would be enough to get a better decomposition analysis of the signal. However, due to the changes in scale, a wavelet transform does not provide a time-frequency representation per se: rather than a frequency axis, it comprises an axis where scales are shown – while being related to frequency, the scale is not linear, so some frequencies are given more weight than others [47]. Resolution also depends on the type of wavelet function used, and therefore, the scale to apply. A mother wavelet that optimally fits the signal depending on the application and the signal itself is difficult to find. In this sense, more complex approaches regarding time-frequency analysis should be borne in mind [47].

Stability of the application could be improved. Although there have not been too many problems regarding this issue, real time analysis in the Matlab is limited. The code could be written instead in C+ and be implemented in a more powerful and fast software, such as Python. It is also important to notice that the proposed analysis platform makes use of only one channel for acquisition of the signal, but it has the capability to make use of up to 5 more channels for acquisition of data (one EKG-EMG shield board by channel). In this sense, the application has the ability to be adapted depending on the number of channels required based on the needs of the researchers at the Unit. Finally, the transfer of data between Arduino-PC could be extended to the use of Wi-Fi for its transmission, taking advantage of the existing network already established at the Langendorff bioreactor for control of the pumps, flows and reservoirs.

7. Conclusions

Quantifying the complexity of the electrocardiographic signals is of great importance to help understand the mechanisms of perpetuation of arrhythmias and to compare the effectiveness of potential drugs used to control the fibrillatory activity.

The main objective of this project was to design, implement and validate a real-time registering and analysis platform for epicardial and endocardial cardiac electrograms for isolated heart models. Ability to automatically detect myocardial rhythm, onset of ventricular fibrillation events and fundamental frequency of the electric signals was paramount:

1. A real-time registering and analysis platform was developed by implementing time and frequency domain algorithms that provided expected results.
    - Search of QRS complex in the time domain, using slope, amplitude and width information of the signal, allowed automatic identification of the myocardial rhythm.
    - Analysis of frequency spectrums allowed automatic characterization of the fundamental frequency of myocardial activations.
    - Analysis of the non-linearity of the electrocardiographic signals by reconstruction of the so-called phase-space allowed discriminating ventricular fibrillation episodes and normal sinus rhythm ECG signals.
2. An electrocardiographic waveform simulator was developed for testing the final platform. It was able to generate epicardial and endocardial signals of interest, providing a powerful method to test the system before ex-vivo experiments were carried out.
3. Ex-vivo experiments of isolated porcine hearts in a Langendorff bioreactor were effective to validate the signals registered with the developed analysis and registering platform: electric recordings were compared with off-line analysis of gold standard records obtained from optical mapping techniques, and correlation between the two was faithfully demonstrated.

To summarize, the developed platform presents a fast, easy and quite accurate approach with which researchers could quantify the complexity of the electrical activity of the heart, as arrhythmias are induced in isolated heart models within a Langendorff bioreactor. The ultimate utility of the project would be to help the researchers at the time of inducing fibrillations to objectify modifications and develop better therapies or maneuvers.

Bibliography

1. Dickstein K, Cohen-Solal A, Filippatos G, McMurray JJV, Ponikowski P, Poole-Wilson PA, et al. ESC Guidelines for the diagnosis and treatment of acute and chronic heart failure 2008. Eur Heart J. 2008 Oct;29(19):2388–442.
2. Ideker RE, Rogers JM. Human ventricular fibrillation: wandering wavelets, mother rotors, or both? Circulation. 2006 Aug 8;114(6):530–2.
3. Jalife J. Ventricular fibrillation: mechanisms of initiation and maintenance. Annu Rev Physiol. 2000;62.
4. Weiss JN, Chen P-S, Wu T-J, Siegerman C, Garfinkel A. Ventricular fibrillation: new insights into mechanisms. Ann N Y Acad Sci. 2004 May;1015:122–32.
5. Everett TH, Moorman JR, Kok LC, Akar JG, Haines DE. Assessment of global atrial fibrillation organization to optimize timing of atrial defibrillation. Circulation. 2001 Jun 12;103(23):2857–61.
6. Villani GQ, Nollo G, Ravelli F, Piepoli M, Capucci A. Capture of atrial fibrillation reduces the atrial defibrillation threshold. Pacing Clin Electrophysiol PACE. 2002 Aug;25(8):1159–65.
7. Scheinman MM. Mechanisms of atrial fibrillation: is a cure at hand? J Am Coll Cardiol. 2000 May;35(6):1687–92.
8. Nanthakumar K, Jalife J, Massé S, Downar E, Pop M, Asta J, et al. Optical mapping of Langendorff-perfused human hearts: establishing a model for the study of ventricular fibrillation in humans. Am J Physiol - Heart Circ Physiol. 2007 Jul 11;293(1):H875–80.
9. Noble RJ, Hillis JS, Rothbaum DA. Electrocardiography. In: Walker HK, Hall WD, Hurst JW, editors. Clinical Methods: The History, Physical, and Laboratory Examinations. 3rd ed. Boston: Butterworths; 1990.
10. Berbari E. Chapter 13. Principles of electrocardiography. The Biomedical Engineering Handbook. Second edition. CPR Press; 2010. p. 500–10.
11. Guyton A, Hall J. Electrocardiographic interpretation of caridac muscle and coronary blood flow abnormalitites: vectorial analysis. Textbook of medical physiology. 11th ed. Elsevier Saunders; 2006. p. 131–47.
12. Guyton A, Hall J. Heart muscle; the heart as a pump and function of the heart valves. Textbook of medical physiology. 11th ed. Elsevier Saunders; 2006. p. 103–16.
13. Tortora G, Derrickson B. The cardiovascular system: the heart. Principles of anatomy and physiology. 13th ed. Jhon Wiley & Sons; 2012. p. 757–801.
14. Jalife J, Delmar M, Anumonwo J, Berenfeld O, Kalifa J. Basic Cardiac Electrophysiology for the Clinician. Second. Wiley-Backwell; 2009. 358 p.
15. Guyton A, Hall J. Rhythmical excitation of the heart. Textbook of medical physiology. 11th ed. Elsevier Saunders; 2006. p. 116–23.
16. Guyton A, Hall J. The normal electrocardiogram. Textbook of medical physiology. 11th ed. Elsevier Saunders; 2006. p. 123–31.

17. Holland K. Atrial Fibrillation vs. Ventricular Fibrillation [Internet]. Healthline. [cited 2015 Apr 25]. Available from: http://www.healthline.com/health/atrial-fibrillation-vs-ventricular-fibrillation#1

18. Ventricular Fibrillation: New Insights for the Healthcare Professional: 2013 Edition: ScholarlyPaper. ScholarlyEditions; 2013. 46 p.

19. Moe GK, Rheinboldt WC, Abildskov JA. A computer model of atrial fibrillation. Am Heart J. 1964 Feb;67(2):200–20.

20. Valentinuzzi ME. Cardiac Fibrillation-Defibrillation: Clinical and Engineering Aspects. World Scientific; 2010. 302 p.

21. Ibañez Catala X. Cuantificación de la complejidad de la fibrillación mediante el aislamiento espacio-temporal de frentes de activación miocárdica. [Valencia]: Universidad de Valencia; 2011.

22. Janse MJ, Moréna H, Cinca J, Fiolet JW, Krieger WJ, Durrer D. Electrophysiological, metabolic and morphological aspects of acute myocardial ischemia in the isolated in the isolated porcine heart. Characterization of the "border zone. J Physiol (Paris). 1980;76(7):785–90.

23. Dixon JA, Spinale FG. Large Animal Models of Heart Failure A Critical Link in the Translation of Basic Science to Clinical Practice. Circ Heart Fail. 2009 May 1;2(3):262–71.

24. Skrzypiec-Spring M, Grotthus B, Szeląg A, Schulz R. Isolated heart perfusion according to Langendorff—Still viable in the new millennium. J Pharmacol Toxicol Methods. 2007 Mar;55(2):113–26.

25. Zimmer H-G. The Isolated Perfused Heart and Its Pioneers. News Physiol Sci Int J Physiol Prod Jointly Int Union Physiol Sci Am Physiol Soc. 1998 Aug;13:203–10.

26. Bell RM, Mocanu MM, Yellon DM. Retrograde heart perfusion: The Langendorff technique of isolated heart perfusion. J Mol Cell Cardiol. 2011 Jun;50(6):940–50.

27. Chorro FJ, Such-Belenguer L, López-Merino V. Animal Models of Cardiovascular Disease. Rev Esp Cardiol Engl Ed. 2009 Jan;62(1):69–84.

28. Schmid O. Untersuchungen am überlebenden Säugetierherzen. 1925. 94 p.

29. Herron TJ, Lee P, Jalife J. Optical imaging of voltage and calcium in cardiac cells & tissues. Circ Res. 2012 Feb 17;110(4):609–23.

30. Laughner JI, Ng FS, Sulkin MS, Arthur RM, Efimov IR. Processing and analysis of cardiac optical mapping data obtained with potentiometric dyes. Am J Physiol Heart Circ Physiol. 2012 Oct 1;303(7):H753–65.

31. Efimov IR, Nikolski VP, Salan G. Optical Imaging of the Heart. Circ Res. 2004;95: 21–33.

32. Attin M, Clusin WT. Basic concepts of optical mapping techniques in cardiac electrophysiology. Biol Res Nurs. 2009 Oct;11(2):195–207.

33. Lee P, Taghavi F, Yan P, Ewart P, Ashley EA, Loew LM, et al. In Situ Optical Mapping of Voltage and Calcium in the Heart. PLoS ONE. 2012 Agosto;7(8):e42562.

34. Arora R, Das MK, Zipes DP, Wu J. Optical Mapping Of Cardiac Arrhythmias. Indian Pacing Electrophysiol J. 2003 Oct 1;3(4):187–96.

35. Efimov IR, Huang DT, Rendt JM, Salama G. Optical mapping of repolarization and refractoriness from intact hearts. Circulation. 1994 Sep 1;90(3):1469–80.

36. Zaitsev AV, Guha PK, Sarmast F, Kolli A, Berenfeld O, Pertsov AM, et al. Wavebreak formation during ventricular fibrillation in the isolated, regionally ischemic pig heart. Circ Res. 2003 Mar 21;92(5):546–53.

37. Amann A, Tratnig R, Unterkofler K. Reliability of old and new ventricular fibrillation detection algorithms for automated external defibrillators. Biomed Eng OnLine. 2005 Oct 27;4(1):60.

38. Ismail AH, Fries M, Rossaint R, Leonhardt S. Validating the Reliability of Five Ventricular Fibrillation Detecting Algorithms. In: Sloten JV, Verdonck P, Nyssen M, Haueisen J, editors. 4th European Conference of the International Federation for Medical and Biological Engineering. Springer Berlin Heidelberg; 2009. p. 26–9.

39. Pan J, Tompkins WJ. A real-time QRS detection algorithm. IEEE Trans Biomed Eng. 1985 Mar;32(3):230–6.

40. Das S, Chakraborty M. Comparison of normal and ventricular tachyarrhythmic electrocardiograms using scatter plots. J Inf Technol. 2012 Apr;2(2):32–7.

41. Thakor NV, Zhu YS, Pan KY. Ventricular tachycardia and fibrillation detection by a sequential hypothesis testing algorithm. IEEE Trans Biomed Eng. 1990 Sep;37(9):837–43.

42. Chen S, Thakor NV, Mower MM. Ventricular fibrillation detection by a regression test on the autocorrelation function. Med Biol Eng Comput. 1987 May;25(3):241–9.

43. Zhang XS, Zhu YS, Thakor NV, Wang ZZ. Detecting ventricular tachycardia and fibrillation by complexity measure. IEEE Trans Biomed Eng. 1999 May;46(5):548–55.

44. Lempel A, Ziv J. On the Complexity of Finite Sequences. IEEE Trans Inf Theory. 1976 Enero;22(1):75–81.

45. Barro S, Ruiz R, Cabello D, Mira J. Algorithmic sequential decision-making in the frequency domain for life threatening ventricular arrhythmias and imitative artefacts: a diagnostic system. J Biomed Eng. 1989 Jul;11(4):320–8.

46. Pal S, Mitra M. Detection of ECG characteristic points using Multiresolution Wavelet Analysis based Selective Coefficient Method. Measurement. 2010 Feb;43(2):255–61.

47. Rosado Muñoz A. Desarrollo de Técnicas de Detección de Fibrilación Ventricular Basadas en Algoritmos Tiempo-Frecuencia. [Valencia]: Universidad de Valencia; 2000.

48. Umapathy K, Nair K, Masse S, Krishnan S, Rogers J, Nash MP, et al. Phase Mapping of Cardiac Fibrillation. Circ Arrhythm Electrophysiol. 2010 Feb 1;3(1):105–14.

49. Lin C-H. Frequency-domain features for ECG beat discrimination using grey relational analysis-based classifier. Comput Math Appl. 2008 Feb;55(4):680–90.

50. Kim SI, Suh TS. A new quantitative analysis technique for cardiac arrhythmia classification using bispectrum and bicoherency. San Francisco, CA, USA: Springer Science & Business Media; 2004. p. 13–6.

51. Minami K, Nakajima H, Toyoshima T. Real-time discrimination of ventricular tachyarrhythmia with Fourier-transform neural network. IEEE Trans Biomed Eng. 1999 Feb;46(2):179–85.

52. Fojt O, Holcik J. Applying nonlinear dynamics to ECG signal processing. IEEE Eng Med Biol Mag. 1998 Mar;17(2):96–101.

53. Amann A, Tratnig R, Unterkofler K. Detecting ventricular fibrillation by time-delay methods. IEEE Trans Biomed Eng. 2007 Jan;54(1):174–7.

54. Amann A, Tratnig R, Unterkofler K. A new ventricular fibrillation detection algorithm for automated external defibrillators. Computers in Cardiology, 2005. 2005. p. 559–62.

55. PocketECG: a new continuous and real-time ambulatory arrhythmia diagnostic method. Cardioloy J. 2011;28(4):454–60.

56. Chorro FJ, Trapero I, Guerrero J, Such LM, Canoves J, Mainar L, et al. Modification of ventricular fibrillation activation patterns induced by local stretching. J Cardiovasc Electrophysiol. 2005 Oct;16(10):1087–96.

57. Chorro FJ, Trapero I, Such-Miquel L, Pelechano F, Mainar L, Canoves J, et al. Pharmacological modifications of the stretch-induced effects on ventricular fibrillation in perfused rabbit hearts. Am J Physiol Heart Circ Physiol. 2009 Nov;297(5):H1860–9.

58. Chorro FJ, Blasco E, Trapero I, Canoves J, Ferrero A, Mainar L, et al. Selective myocardial isolation and ventricular fibrillation. Pacing Clin Electrophysiol PACE. 2007 Mar;30(3):359–70.

59. Rogers JM, Huang J, Pedoto RW, Walker RG, Smith WM, Ideker RE. Fibrillation is More Complex in the Left Ventricle than in the Right Ventricle. J Cardiovasc Electrophysiol. 2000 Dec 1;11(12):1364–71.

60. Chattipakorn N, Fotuhi PC, Chattipakorn SC, Ideker RE. Three-dimensional mapping of earliest activation after near-threshold ventricular defibrillation shocks. J Cardiovasc Electrophysiol. 2003 Jan;14(1):65–9.

61. Rocha T, Paredes S, de Carvalho P, Henriques J, Antunes M. Phase space reconstruction approach for ventricular arrhythmias characterization. 30th Annual International Conference of the IEEE Engineering in Medicine and Biology Society, 2008 EMBS 2008. 2008. p. 5470–3.

List of tables and figures

Tables

Figures

Appendix I – Electrocardiography waveform generator

Physical implementation

For the correct functioning of the device, follow the instructions listed below:

Fig. 50 USB 2.0 printer cable

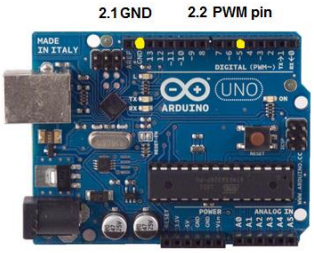

Fig. 51 Arduino UNO

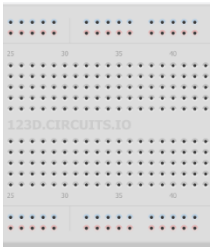

Fig. 52 Protoboard

Fig. 53 Electric cable

- Connect the USB cable to the PC, and plug it to the Arduino UNO board as well.
- Connect the electric cable with the PWM pin on the Arduino board and with the RC low-pass filter on the protoboard. Connect the ground of the circuit to that of the Arduino (see Fig. 54).

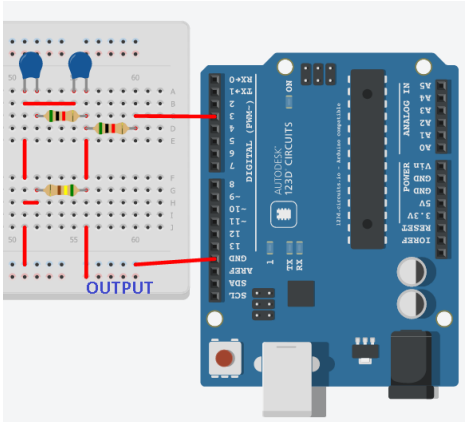

Fig. 54 Arduino UNO + RC low pas filter

Using the software

Software managing:

Once the circuit is correctly mounted, it can be used.

- Start the Arduino IDE software, compile and run the corresponding code SEND_MATLAB_ARDUINO.ino onto the Arduino UNO board (Set Tools - > Board -> Arduino UNO; Set Tools -> Serial Port -> COM3).
- Make sure the monitor serial of Arduino remains close.
- Open Matlab and run the code GENERATOR_GUI.m.

Software interface:

Once the Matlab code is run, the user interface (Fig. 55) will appear:

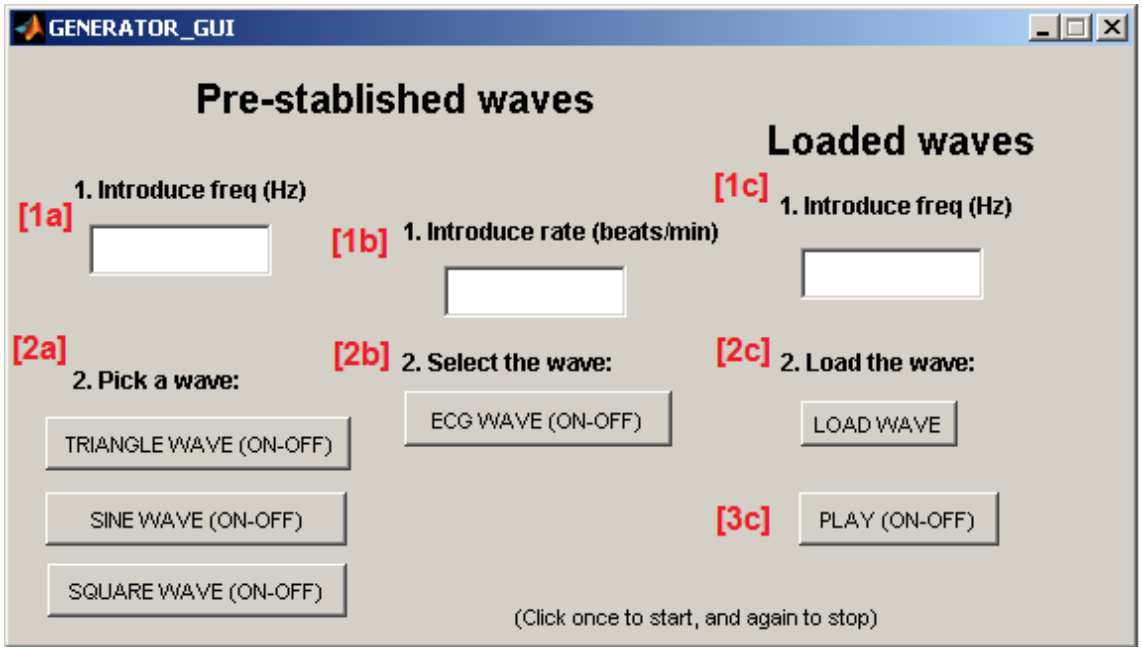

Fig. 55 Electrocardiography waveform simulator interface GUI in Matlab

1. Introduce the frequency in Hz (1a, 1c) or the rate (1b) of the signal.
2. Select a wave (2a: triangle, sine or square; 2b: ECG; 2c: load wave of interest).
3. Run loaded wave.

How to use the application

There are two major options to start using the simulator device: to run pre-established waves (triangle, sine, square or a SNR ECG signal), or to run loaded waves of interest.

- The frequency (1a, 1c) or rate (1b) of the signal with which you want to generate the wave must be introduced in the corresponding cell. Once a signal has been chosen (2a, 2b), the system starts generating it. In case of loading a wave of interest (2c), a pop-up window will appear where you can select the file containing the signal to load, and afterwards the play button (3c) must be pressed.

- To stop the simulator, click again on the selected wave (2a, 2b) or on the play button (3c).

Appendix II - Electrocardiography registering and analysis platform

Physical implementation

For the correct functioning of the platform, follow the instructions listed below:

Fig. 56 USB 2.0 printer cable

Fig. 57 Catheter

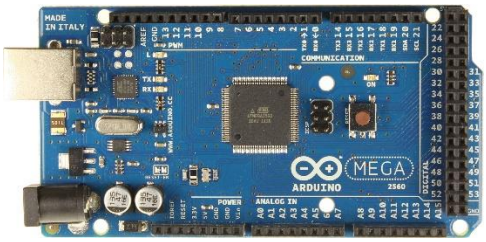

Fig. 58 Arduino Mega2560

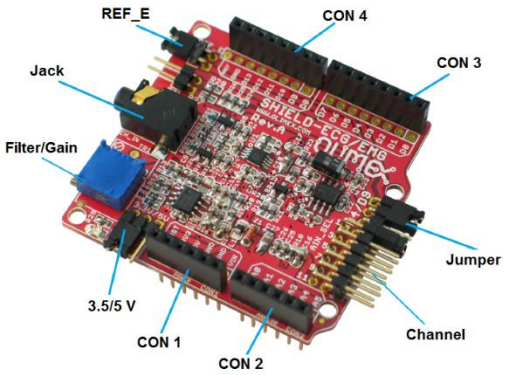

Fig. 59 EKG-EMG board

- Connect the USB cable to the PC, and plug the other end to the Arduino Mega2560 board.
- Set the EKG-EMG shield in the following way:
  - REF_E: closed position.
  - 3.3/5 V: 5V position.
  - Jumper: D9 position.
  - Channel: select the number of channels.
- Place the EKG-EMG shield on top of the Arduino board. The EKG-EMG shield will be powered by the host board it is mounted on. Make sure that the shield is correctly mounted on top of the Arduino device.
- Connect the catheter or the waveform simulator connector to the Jack connection on the EKG-EMG board.

Using the software

Software managing:

Once the circuit is correctly mounted, it can be used:

- Start Arduino IDE software and open the corresponding project file.ino.
- Compile and run the code onto the corresponding board: Set Tools - > Board -> Arduino Mega 2560; Set Tools -> Serial Port -> COM8.
- Make sure the monitor serial of Arduino remains close.
- Start Matlab software and run the project GUI file.

Software interface:

After running the code, the user interface (Fig. 60) will appear:

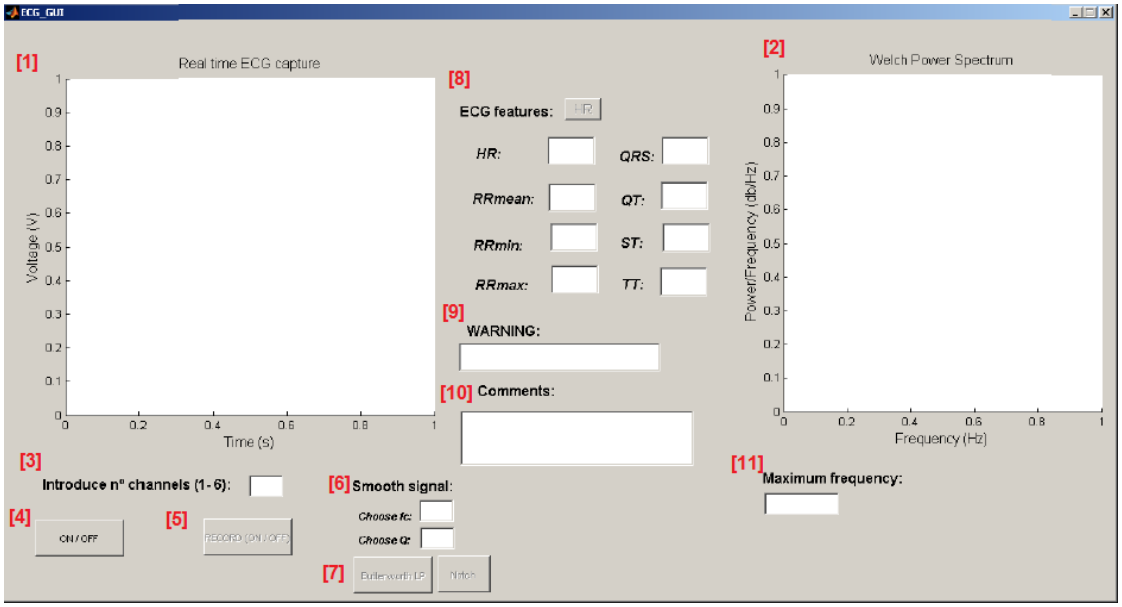

Fig. 60 Electrocardiography analysis platform user interface GUI in Matlab

1. Real-time ECG capture.
2. Real-time power spectrum.
3. Number of channels.
4. ON/OFF button
5. Record signal.
6. Smooth signal.
7. Butterworth LP/ Notch filter.
8. HR button: ECG features.
9. Warning: VF episodes.
10. Introduce comments.
11. Maximum frequency.

How-to use the application:

Turning on/off the device

To start using the application, the first thing to do is to specify the number of channels (3), and subsequently press the start ON/OFF button (4).

Once the start button has been pressed, the rest of functionalities will get enabled for their use, and the electrocardiographic signal (1) and corresponding power spectrum (2) will be displayed in the figures in real-time.

To stop the application, the ON/OFF (4) button should be pressed again.

Analysis functionalities

By pressing the HR button (8), characteristic parameters of the signal of interest will be computed and their values will appear (hear rate, QRS interval, mean RR interval, and so on).

The fundamental frequency of the signal will be displayed in the power spectrum, and its value will be computed (11).

Normal sinus rhythm ECG signals will be discriminated from ventricular fibrillation episodes, and the corresponding warning will be shown (9).

Notice that in case too much noise appears, two different filters (7) can be applied to the signal (Butterworth LP or Notch):

- For the Butterworth LP, the cutoff frequency in Hz must be written down (8), and it will be normalized by the internal algorithm. Otherwise, a pre-established value will be used.
- For the Notch filter, the quality factor Q must be written down (8) so that the bandwidth BW can be calculated. Otherwise, a pre-established value will be used.

Recording the signal

To record the signal being acquired in real-time, press the Record button (5). The functionality will be only enabled once the application is turned on.

Signals will be saved online into a corresponding folder named Recordings in the specified directory, ordered by creation date. The recording signal will be saved into two configurations:

- A structure.mat file containing the information of the study, which can be useful for its further offline processing in Matlab.
- A .txt file that can be exported to other software applications such as NotePad, Excel, Word…

Comments can also be written in the corresponding box (10) as the signal is being saved. Comments will be added to the .txt file at the precise time they have been noted down.

During each continuous study, the signal can be recorded as many times the user desires. Each time, a new structure.mat will be generated, and the .txt file will be updated with the new information. To differentiate a new recorded signal in the .txt file, a new header will appear.

By pressing the Record button (5) again, the implementation will be turned off and the singal/comments will be no longer saved.

Appendix III – Optical mapping analysis

Using the software

Software interface

Open Matlab and run the program. The user interface will appear (Fig. 61):

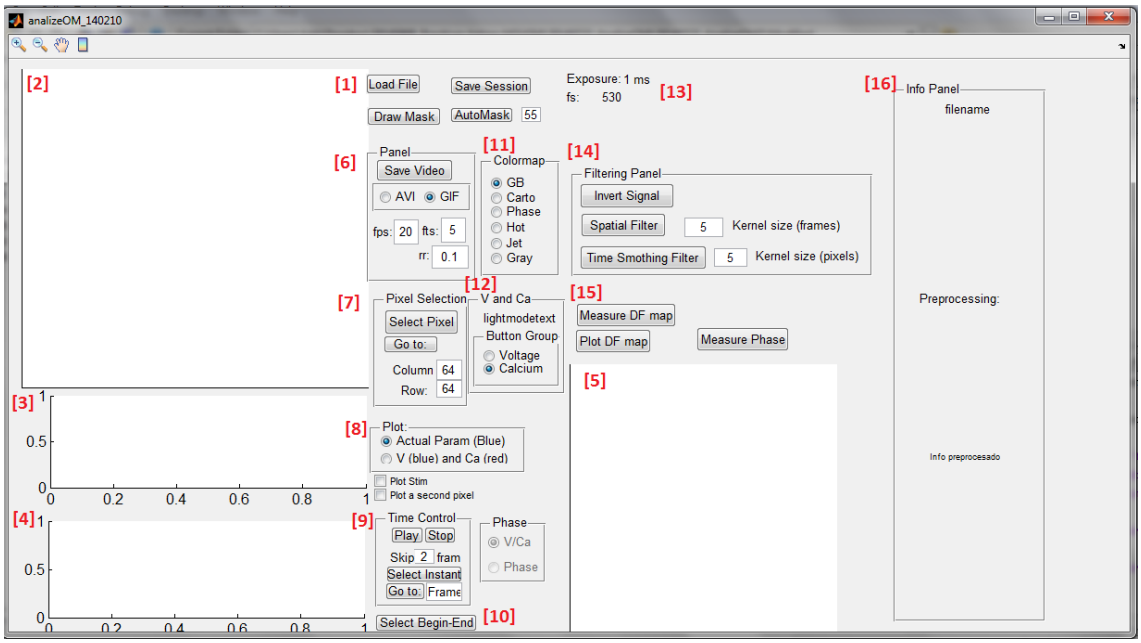

Fig. 61 AnalizeOM (Optical mapping analysis) user interface GUI in Matlab.

1. Starting buttons: load file, draw mask/automask, save session.
2. Image of the sample under study.
3. Voltage/Calcium signal (depolarization/repolarization).
4. Welch's power spectrum.
5. Dominant Frequency map.
6. Panel to record a video.
7. Panel selection: select pixel of interest.
8. Plot panel: voltage/calcium parameter.
9. Time control panel: play/stop, select instant of interest/go to specific frame.
10. Select begin-end (cut the sample of interest).
11. Colormap.
12. Voltage/Calcium.
13. Image information (exposure, sampling frequency).
14. Filtering panel (invert signal, spatial filtering, time smooth signal).
15. DF map features.
16. Information panel.

How to use the application:

Preparing the sample

To start using the application, the first thing to do is to load the file of interest (1) that needs to be analyzed. Click on “select pixel” (7) and then on the black box that appears (2) to show the image of the sample under study.

Once the image is shown in the figure (2), the next step is to select the region of interest for analysis – this will save time for image processing and analysis. This can be done by drawing a mask manually or automatically (1).

Filtering (14) must be performed too (kernel sizes can be selected). This will normalize the signal and reduce noise. First, a spatial filtering, and then a time smoothing. The signal should be inverted to be placed in the correct position too. Now, the sample is ready to be analyzed.

Analysis functionalities

By selecting a pixel (7) of interest within the image, the voltage signal trace will appear (3) along with the fundamental frequency value in the Welch’s power spectrum (4). To obtain the calcium signal trace at such pixel, select the calcium parameter (12). Signal traces between selected points can be obtained by selecting a starting and ending points within the signal trace (10).

The voltage-calcium signal can be observed simultaneously by selecting the V/Ca option (8).

The colormap menu (11) enables to visualize the current sample at different color options.

The Dominant Frequency map can be calculated (15) and shown in the corresponding figure (5).

The time control menu (9) allows the playback of the recorded video. A red circle on the signal trace (3) is made visible indicating the point of the time video.

Recording the study

The study session can be saved (1) and a video of the propagation of the electric signal within the cardiac tissue substrate can be recorded (6). The format can be selected (.AVI, .GIF), as well as the frames per second.